Chapter – IV

Geochemical evolution of the Mesoproterozoic Chhattisgarh Basin

4.1 Introduction

The Mesoproterozoic Era was largely considered as an uneventful period in the history of evolution of the Earth, and is often tagged as ‘the boring billion’ for the remarkable stability in its carbon isotope record and the lack of any major global glaciations like the ones occurred in the preceding and succeeding eras (Brasier and Lindsay, 1998). A number of recent studies, however, suggest a consistent increase in the $\delta^{13}C$ of the marine carbonates up to +4‰ globally, towards terminal Mesoproterozoic, though the reasons for this trend remain unclear (Bartley et al., 2001; Bartley and Kah, 2004; Kah et al., 2012). The ocean bottoms remained largely anoxic with pockets of euxinia at restricted basin margins and biologically productive regions, while the atmospheric oxygen levels have likely remained < 0.01 times of the present atmospheric levels (Lyons et al., 2014). Besides, the Mesoproterozoic has also witnessed the dismantling of the supercontinent Columbia following its maximum packing at ~1.45 Ga, and the beginning of amalgamation of the early Neoproterozoic Rodinia (Meert and Santosh, 2017). The deposition of the Chhattisgarh Supergroup occurred during this time period. Deposited largely over the ~2.5 Ga granitoids of the Baster craton, the Supergroup consists chiefly of undeformed and unmetamorphosed fluvial and marine siliciclastics, carbonates, and volcaniclastics. The sedimentation in the basin began around 1.45 Ga (Das et al., 2011) and continued at least up to 1.0 Ga (Patranabis-Deb et al., 2007), forming 2.2 – 2.5 km thick repository of sediments, which hold clues to our understanding of the Mesoproterozoic oceans as well as the tectono-climatic evolution of the Indian shield subsequent to the break-up of the Columbia.

4.2 Objectives

The specific objectives of the present work were to,

1. Establish the chronology of deposition of various carbonate formations in the basin using $\delta^{13}C$ chemostratigraphy and Sr isotope stratigraphy.

2. Unravel the sedimentary history of the basin and the tectonic setting by quantitative provenance analysis of the siliciclastics from sandstone, shale and carbonate formations, and volcaniclastics using trace element and Nd isotopic ratios.

3. Better understand the dynamics of the Mesoproterozoic Ocean using stable carbon and oxygen isotopes study of both limestone and dolostone formations of the Chhattisgarh Supergroup.

4.3 Geological Setting

4.3.1 Regional Geology

The Bastar Craton of the central India is bounded by the Godavari and Mahanadi grabens in the south and northeast, respectively, whereas the Central Indian Tectonic Zone (CITZ), a part of the Satpura Mobile Belt (SMB), demarcates its northern boundary, and Eastern Ghats Mobile Belt (EGMB) borders the craton in the southeast (Fig. 4.1 A). The craton encompasses of a blend of volcano-sedimentary rift basins formed from Mesoarchean to Paleoproterozoic, essentially consisting of Archaean and Paleoproterozoic granites with isolated enclaves of banded Tonalite-Trondhjemite Granodiorite (TTG) gneisses, with some of them as old as ~3.5 Ga (Ghosh, 2004), and low- to high-grade metasediments consisting of quartzite-carbonate-pelite (QCP) with Banded Iron Formation (BIF) and minor mafic-ultramafic rocks as supracrustals within these gneisses. The supracrustal enclaves, called the Sukma Group in the south and Amgaon Group in the north, are overlain by the quartzite-basalt-pelite succession of the 2.5-2.6 Ga Bengpal Group (Ramakrishnan and Vaidyanadhan, 2010). Paleoproterozoic BIF basins, e.g., the Bailadila Group, unconformably overlie the Bengpal Group, as well as the basement granites and gneisses with the Sukma and Amgaon enclaves. They are overlain by the volcano-sedimentary sequence of the Kotri-Dongargarh orogen starting with the argillaceous Dargarh Group, followed by basalt, basaltic andesite, rhyolite and pyroclastics dominated Nandgaon Group of 2.47 Ga and the basalt-sandstone alternate succession of the Kairagarh Group. The low grade metasediments of the Chilpi Group overlie the volcano-sedimentary unit. This volcano-sedimentary sequence is intruded by the 2.43 Ga Dongargarh Granite. Bimodal volcanics, BIF and greywacke-argillite dominated Sonakhan, and pelites, bimodal volcanics and pyroclastics dominated Sakoli occur as isolated fold belts within the gneisses in the east and west of the Kotri-Dongargarh belt (Sharma, 2009). The craton attained stability by Paleoproterozoic which facilitated formations of the Mesoproterozoic Chhattisgarh, Indravati and Khariar basins and depositions of marine and continental sediments in them.

4.3.2 Geology of the Chhattisgarh basin

The sediments of the Chhattisgarh basin, called the Chhattisgarh Supergroup, lie unconformably over the basement complex of Archean-granites and gneisses with associated metasediment and metavolcanic rocks of the Sonakhan Greenstone Belt (SGB), and Chilpi Group, covering an area of about 33000 km^2 (Murti, 1987) (Fig. 4.1 B) . The Kotri-Dongargarh fold belt, Mahanadi Graben, and the Eastern Ghats Mobile Belt (EGMB) form boundaries of the basin at west, northeast, and the southeast, respectively. The north and the northwest of the basin are bound by the Central Indian Tectonic Zone (CITZ), which hosts the late Paleoproterozoic Tirodi Biotite Gneiss (TBG) and Ramakona-Katangi mafic Granulite (RKG) belt, the unclassified gneiss south of TBG and the Neoarchean Balaghat-Bhandara mafic Granulite (BBG) belt along with the Paleoproterozoic Mahakoshal Group (Ramakrishnan and Vaidyanadhan, 2010). The ~2500 m thick sedimentary sequence of the Chhattisgarh Supergroup is deposited over two sub-basins – the Hirri in the west and Bharadwar in the east, separated by Sonakhan Greenstone Belt (SGB), and two proto-basins in the southeast – the Singhora and Barapahar (Das et al., 1992). Lithostratigraphically, Chhattisgarh Supergroup itself is divided into four groups– the Singhora, Chandarpur, Raipur and the Kharsiya in temporally ascending order (Mukherjee et al., 2014) (Fig. 3.2).

Sedimentation in the Chhattisgarh basin got initiated in the eastern part where the basal Singhora Group was deposited in the two proto-basins, the Singhora and Barapahar on the Sambalpur Granites. They are largely made up of fluvial sediments consisting of immature sandstone and conglomerate of the Rehatikhol Formation followed by the argillo-calcareous shelf sediments and tuff of the Saraipalli Formation, and the associated sandstone unit of the Bhalukona Member (Das et al., 1992). The status of the Singhora Group within the Chattisgarh basin was ardently debated until lately. Two schools of thought existed – one that argued that the Group was an extension of the basal Chandarpur Group, whereas the other argued in support of the conventional independent group status of the Singhora (Chakraborty et al., 2015). However, a new lithostratigraphic classification of the Supergroup based on a

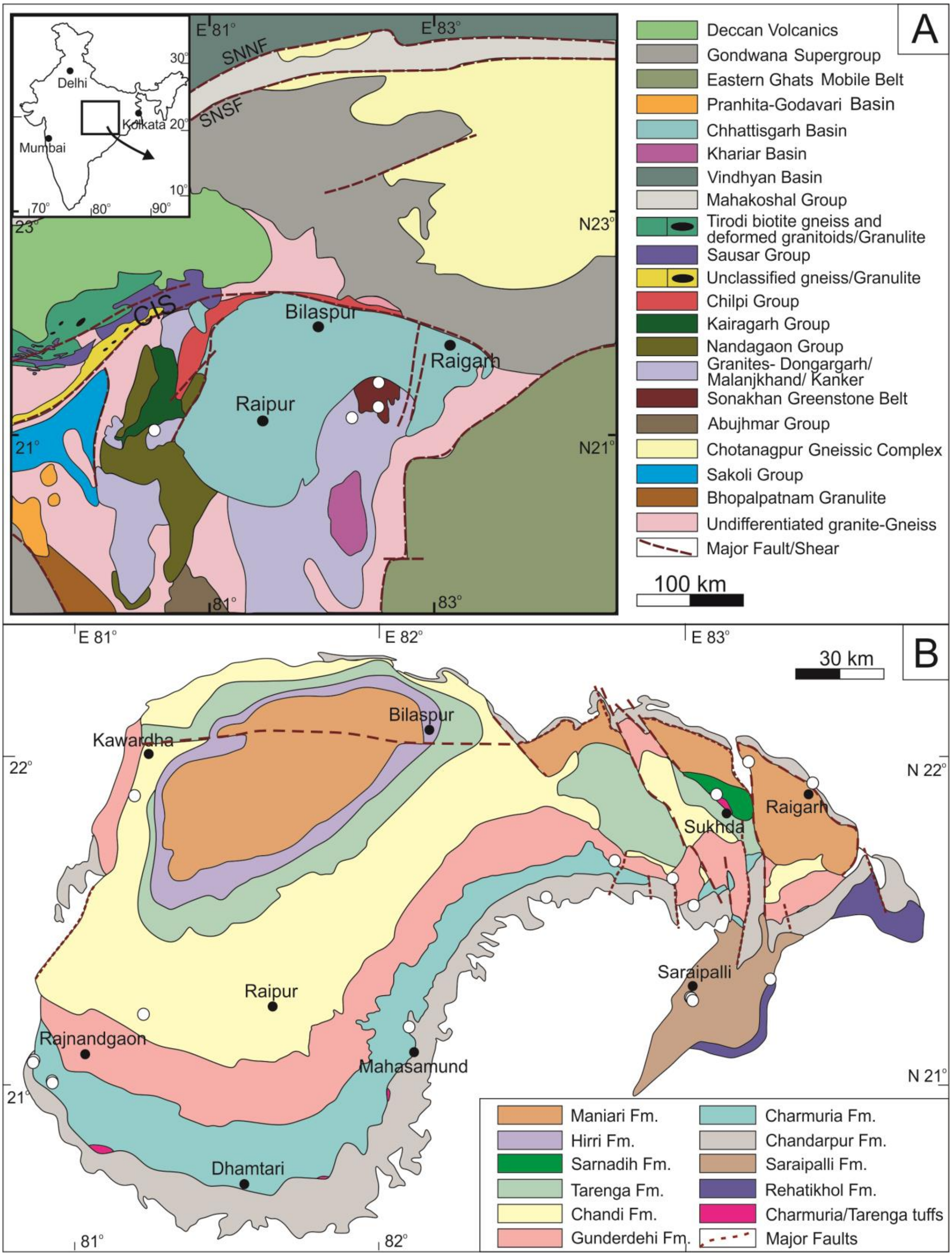

Figure 4.1: (A) Geological map of central India showing Chhattisgarh Supergroup and surrounding litho-tectonic units (modified after Saha and Patranabis-Deb, (2014)). CIS – Central Indian Shear, SNNF – Son Narmada North Fault, SNSF – Son Narmada South Fault. (B) Geological map of the Chhattisgarh Supergroup with stratigraphic subdivisions (modified after Mukherjee et al., (2014)). Sampling locations are marked in white circles.

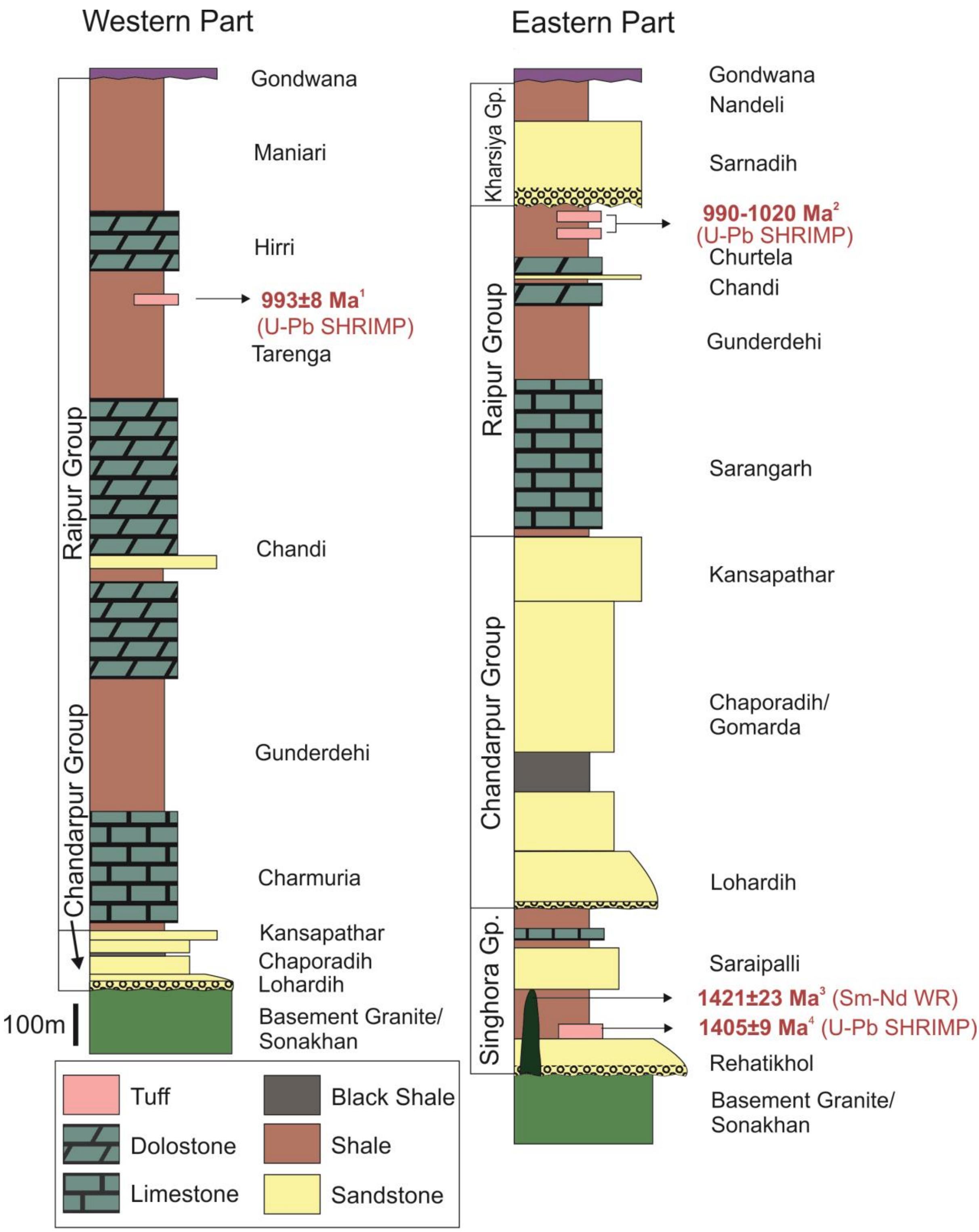

Figure 4.2: Simplified stratigraphy of the Chhattisgarh Supergroup based on information given in Mukherjee et al., (2014), Das et al., (1992), Chakraborty et al., (2015). Ages: [1]Bickford et al., (2011b), [2]Patranabis-Deb et al., (2007), [3]Das et al., (2011), [4]Bickford et al., (2011a). Errors in U-Pb ages are 1σ and Sm-Nd age is 2σ.

number of borehole data now recognizes all the four Groups with minor modifications to the individual members (Mukherjee et al., 2014).

The sedimentation in the basin relapsed with the deposition of the matrix- supported polymictic conglomerate and immature sandstone of the Lohardih Formation, and succeeded by the sandstone-shale dominated Chaporadih (Gomarda) Formation and shallow marine glauconitic sandstone deposit of the Kansapathar Formation. This constitutes the Chandarpur Group (Das et al., 1992). Raipur Group conformably overlies the Chandarpur Group and was deposited by three carbonate-shale cycles. The lower Charmuria (Sarangarh) Formation commences with Sirpur Member shale followed by thick deposits of flaggy limestone (Fig. 4.3) and an upper member of pelagic limestone that grades into the calcareous shale dominated Gunderdehi Formation. Stromatolitic limestone/dolostone makes up most of the overlying Chandi Formation (Fig. 4.4) along with minor sandstone-shale units from the Deodongar Member. The Tarenga (Churtela), Hirri and Maniari Formations overlie the Chandi Formation. They are mostly constituted by dolostone-shale, stromatolitic dolomite and black shale, and gypsiferous purple shale and dolomite, respectively (Das et al., 1992; Murti, 1987). The Tarenga Formation also hosts the Damda tuff in the western Chhattisgarh basin whereas; its contemporaneous Sukhda tuff (Fig. 4.5) is hosted by the Churtela Formation in the eastern Chhattisgarh. A sandstone unit with basal conglomerate unconformably overlies the Churtela Formation in the eastern Bharadwar sub-basin followed by a shale dominated Nandeli Formation. They form the newly constituted Kharsiya Group which is developed only in the Bharadwar sub-basin (Mukherjee et al., 2014).

4.3.3 Chronology of sedimentation

Most of the biostratigraphic studies carried out in the Chhattisgarh basin have ascertained a Meso-Neoproterozoic age for its deposition. Moitra (2003) suggested a late Neoproterozoic age for the topmost Raipur Group based on the stromatolitic assemblages. This argument was supported by the microfossil assemblage of acritarchs and benthic cyanobacteria of different families recovered from the Saradih Formation of the Raipur Group (Singh and Babu, 2013). Singh and Sharma (2016) reported organic walled microfossils dominated by *Leiosphaeridia* from the basal Chandarpur Group and proposed a Meso-Neoproterozoic age for the Chhattisgarh Supergroup.

Initiation of the sedimentation in the Chhattisgarh basin is well constrained. A porcellanite formation sandwiched between the Rehatikhol and Saraipalli formations of the basal Singhora Group has yielded a U-Pb SHRIMP zircon age of 1405±9 (1σ) Ma (Bickford et al., 2011a) and U-Pb EPMA monazite age of ~1500 Ma (Das et al., 2009). Also, Das et al., (2011) reported a Sm-Nd whole rock isochron age of 1421±23 (2σ) Ma for a diabasic intrusive in the Saraipalli Formation. These ages indicate that the sedimentation in the

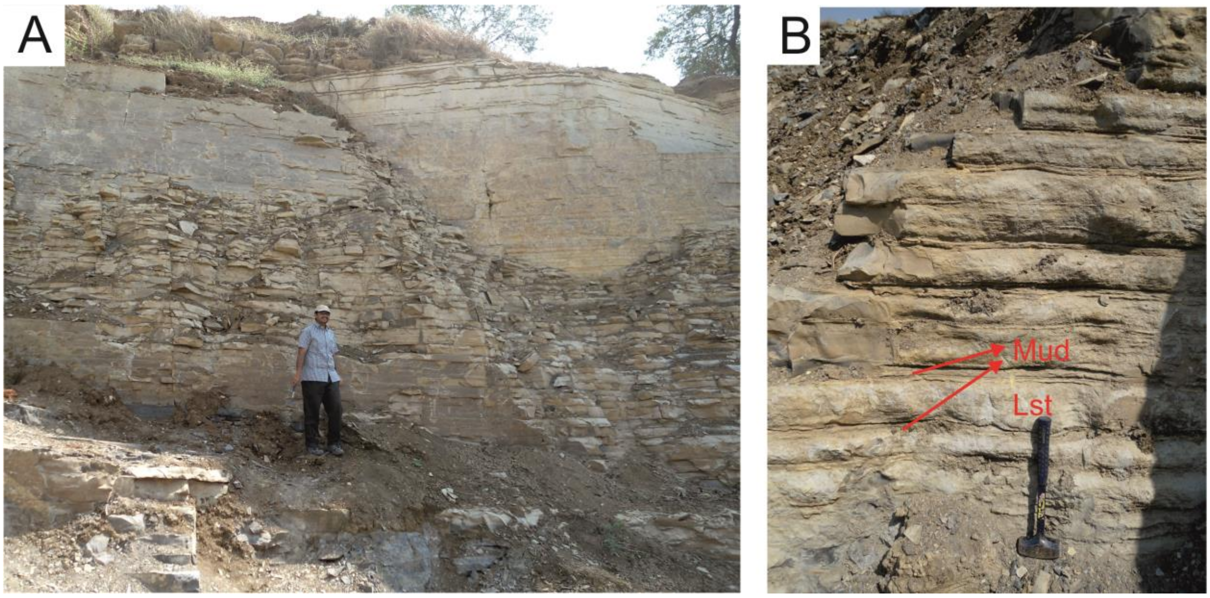

Figure 4.3: (A) Field photograph of the Charmuria Limestone at Gordha village, western Chhattisgarh. (B) A close up outcrop photo showing rhythmic layers of limestone and mud/shale.

Figure 4.4: A close-up outcrop photo of stromatolitic Chandi Dolostone, western Chhattisgarh.

Chhattisgarh basin got initiated before 1.42 Ga. Pandey et al., (2012) attempted to constrain the Chhattisgarh sedimentation by the radiometric dating of the Damdama dolerite dyke which intrudes the Chandarpur Group and provided a Sm-Nd isochron age of 1223±140 (2σ) Ma. However, the date appears to be a mixing line rather than the age of the dyke (Absar, 2013). This is further substantiated by the very low initial $^{143}Nd/^{144}Nd$ (0.51074) displayed by the dolerite dyke. Magmatic zircons from the Sukhda tuff deposited above the Churtela

Formation in the Bharadwar sub-basin and the correlated Damda tuff of the Tarenga Formation in the Hirri sub-basin at the top of Raipur Group yielded U-Pb ages in the range of 990-1020 Ma and 993±8 Ma, respectively, establishing that majority of the deposition happened during the Mesoproterozoic (Bickford et al., 2011b; Patranabis-Deb et al., 2007).

Detrital zircon analysis carried out in the basal Chandarpur sandstones gave a single major peak at ~2500 Ma, which is the age of the basement. However, the Sarnadih sandstone from the top Kharsiya Group yielded a variety of ages ranging from 1006 Ma to 2495 Ma, which constrains the maximum age of the Formation to ~1006 Ma (Bickford et al., 2011a).

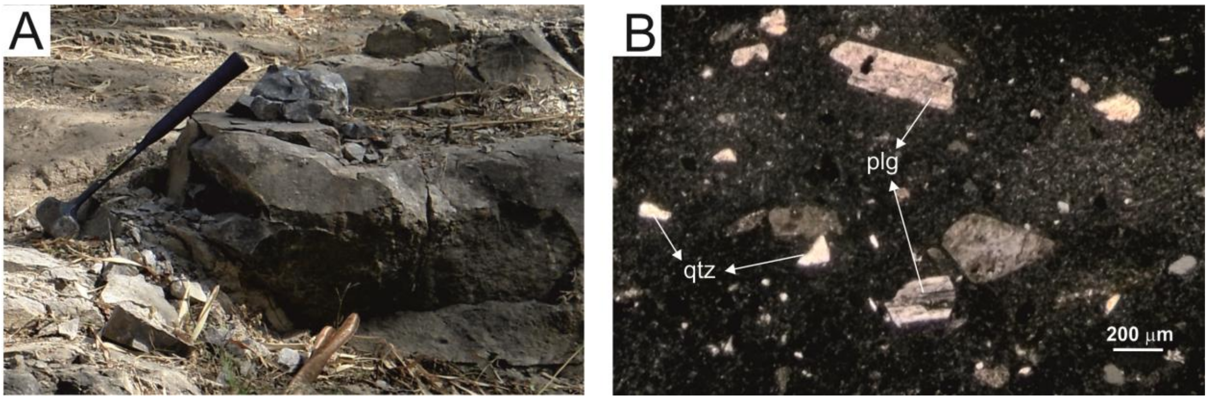

Figure 4.5: (A) Outcrop photo of the Sukhda Tuff near Sukhda village, eastern Chhattisgarh. (B) Photomicrograph of the tuff under cross polarized transmitted light showing angular fragments of plagioclase and quartz.

4.4 Samples and methods

The Charmuria and the Chandi carbonate sequences of the Raipur Group were sampled from quarries near Gordha village, south of Rajnandgaon, and from a quarry located south of Kawardha, respectively, located at the western fringes of the Chhattisgarh basin. Sukhda Tuff was collected from a canal near Sukhda village. We carried out extensive field work and sampling of siliciclastic sedimentary rocks and volcaniclastics from both Hirri and Bharadwar sub-basins and Singhora proto-basin. Samples were also collected from the potential source regions of the sediments such as Basement granitoids and gneisses of the Baster Craton including Kotri-Dongargarh fold belt, Sonakhan Greenstone Belt, and Kairagarh Group. A list of samples with their locations and descriptions are given in Table 4.1. A brief account of the sample preparation protocols and various analytical techniques employed is given in Chapter – 2, and will not be discussed here.

4.5 Results

The carbon and oxygen isotopic composition and trace element data of the Raipur carbonates are presented in Table 4.2. The success of chemostratigraphy lies in extracting the primary geochemical signals from the carbonate samples which are considered to be the representatives of the primordial seawater from which they were precipitated. These primordial compositions get altered when the limestone interacts with secondary meteoric fluids and recrystallize. Over the course of time, a number of petrographic and geochemical techniques have been developed in order to gauge the extent of alteration of the primary signals of carbonates. Carbon isotopic composition of the carbonate samples is generally resilient to alteration by fluids unlike oxygen isotopic composition. However, we have utilized various trace and major element ratios such as Mn/Sr, Ca/Sr, and Mg/Ca and $\delta^{18}O$ to assess the pristine nature of $\delta^{13}C$ compositions.

4.5.1 $\delta^{13}C$ and $\delta^{18}O$ of the Raipur carbonates

The $\delta^{18}O$ of the Charmuria and the younger Chandi limestones vary from -7.9 to -7.4 ‰ and -8.9 to -6.5 ‰, respectively, consistent with the Proterozoic carbonates reported elsewhere (Figs. 4.6 and 4.7). These values are > -10 ‰, the empirically constrained $\delta^{18}O$ below which the $\delta^{13}C$ of the samples are considered altered (Knoll et al., 1995). The Mg/Ca of the Charmuria samples ranges from 0.02 to 0.07 (Fig. 4.6 B). Similarly, bulk of the Chandi Limestone samples displays Mg/Ca between 0.04 and 0.08 (Fig. 4.7 B). Both Charmuria and Chandi limestones display Mn/Sr from 1.2 to 3.4 and the ratios appear scattered when plotted against $\delta^{18}O$ (Figs. 4.6 A and 4.7 A). The low Mn/Sr (< 10) and higher $\delta^{18}O$ (> -10 ‰) suggests that secondary processes could not have altered the primary C isotope signature of the samples (Knoll et al., 1995). $\delta^{13}C$ of the Charmuria and Chandi limestones vary from 2.6 to 3.6 ‰, and 3.2 to 3.6 ‰, respectively (Figs. 4.6 D and 4.7 D), which represent that of the contemporary seawater from which the carbonates precipitated.

4.5.2 $^{87}Sr/^{86}Sr$ of the Raipur carbonates

There are indications, however, that the Sr isotope systematics of both the Charmuria and the younger, Chandi limestones could be disturbed. A slightly higher Mn/Sr than the empirically proposed value of 1.5, below which the $^{87}Sr/^{86}Sr$ of the samples are considered pristine (Knoll et al., 1995), is prevalent in both the limestone formations, suggesting the Sr isotope system of the samples could be disturbed, in spite of the fact that the samples have relatively high Sr concentrations (226 – 617 ppm) (Figs. 4.6 A and 4.7 A). $^{87}Sr/^{86}Sr$ of the

Charmuria Limestone varies from 0.7072 to 0.7086 and that of the Chandi varies from 0.7082 to 0.7137. These ratios when plotted against Ca/Sr appear scattered and did not show the expected linear relationship (Figs. 4.6 C and 4.7 C). The lowest $^{87}Sr/^{86}Sr$ values of the Charmuria and the Chandi limestone formations, 0.7072 and 0.7082, respectively, are more radiogenic than the reported Mesoproterozoic seawater ratios (Shields and Veizer, 2002) and therefore, cannot be used for constraining the ages of depositions of these formations. Two of the Chandi samples (CH 15-30, 40) display low Ca/Sr, but have high $^{87}Sr/^{86}Sr$. This is generally due to the decrease in the Ca content of the samples, rather than high Sr concentrations, and happens as a result of increased dolomitization of the samples (Ray et al., 2003). The relatively high Mg/Ca of these samples, 0.43 and 0.26, respectively, also attests to this. Similarly, three samples of the Charmuria Limestone (CH 15-56, 71, 75) show low Ca/Sr with more radiogenic Sr.

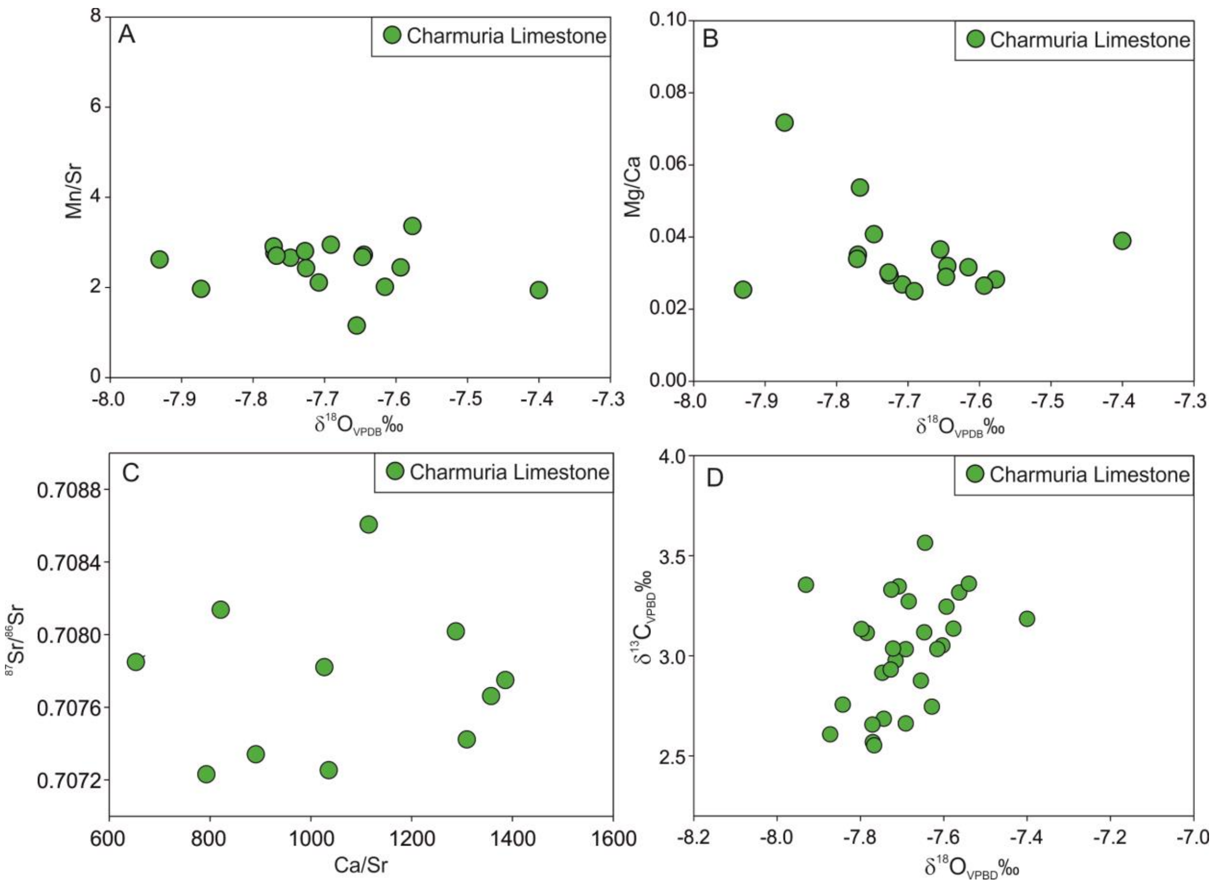

Figure 4.6: Plot of (A) Mn/Sr versus $\delta^{18}O$, (B) Mg/Ca versus $\delta^{18}O$, (C) $^{87}Sr/^{86}Sr$ versus Ca/Sr and (D) $\delta^{13}C$ versus $\delta^{18}O$ for samples from the Charmuria Limestone.

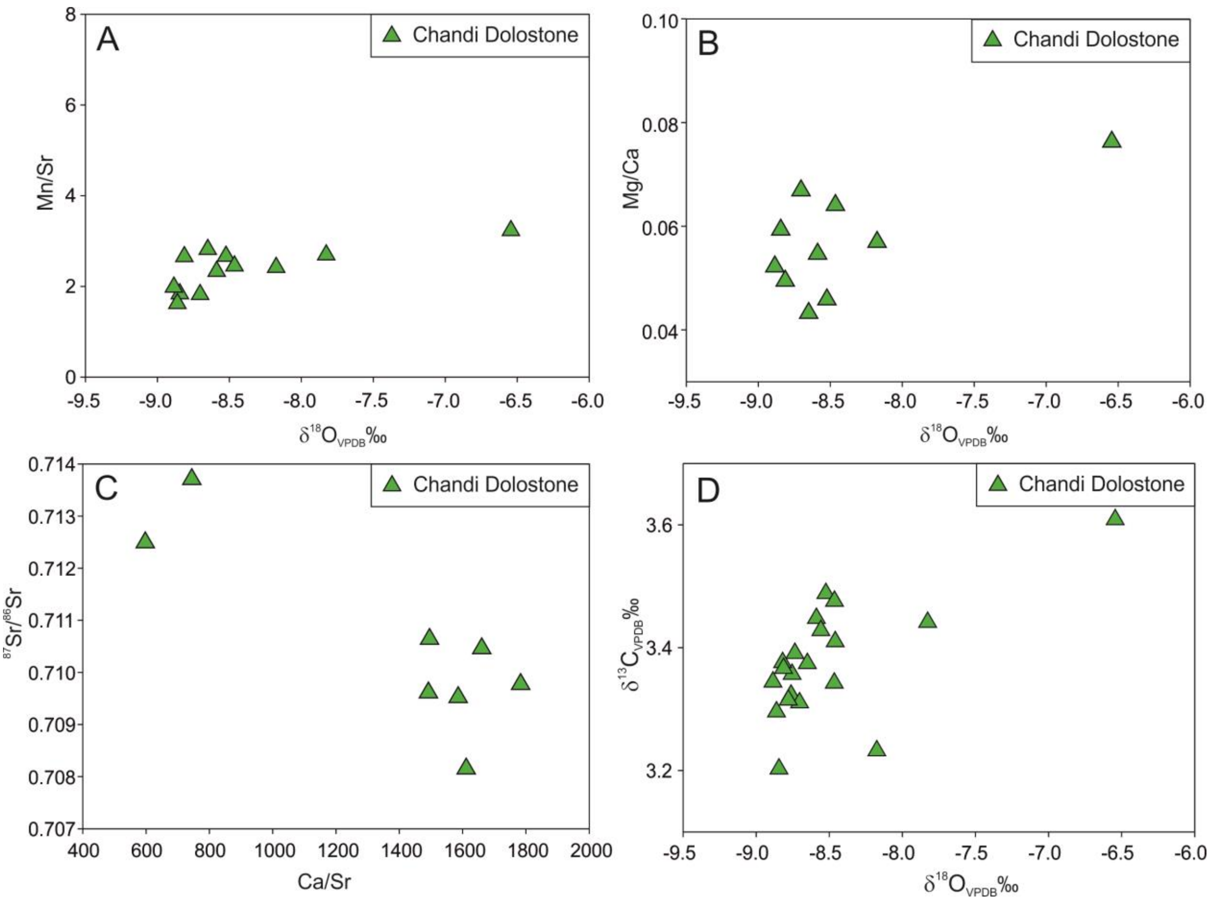

Figure 4.7: Plot of (A) Mn/Sr versus $\delta^{18}O$, (B) Mg/Ca versus $\delta^{18}O$, (C) $^{87}Sr/^{86}Sr$ versus Ca/Sr and (D) $\delta^{13}C$ versus $\delta^{18}O$ for samples from the Chandi Limestone.

4.5.3 Trace element geochemistry

Trace element and isotopic data for the siliciclastic sediments and volcaniclastics from the Chhattisgarh Supergroup are presented in Table 4.3 and are plotted in Figs. 4.8 A and B. The siliciclastic samples display Nb, Ta, Sr, and Eu depletions and Th, U and Pb enrichments when normalized with Primitive Mantle. They also show LREE enriched patterns with La_N/Yb_N ranging from 1.7 to 37.3. The HREE patterns remain nearly flat with Gd_N/Yb_N of the sediments range from 0.91 to 2.69. Pronounced negative Eu anomalies are observed in the samples with an average [Eu/Eu*] of 0.59. A poorly sorted arkosic sandstone from the bottommost Rehatikhol Formation, however, display a positive Eu anomaly ([Eu/Eu*] = 3.4), La_N/Yb_N = 1.7, and Gd_N/Yb_N = 0.57. The remaining Singhora Group samples show La_N/Yb_N from 6.0 to 10.3, whereas the Chandarpur, the Raipur, and the Kharsiya Groups have values in the range of 5.7 to 37.3, 5.2 to 17.6, and 9.0 respectively. Similarly, the Gd_N/Yb_N of the samples varies from 1.02 to 1.28, 0.97 to 2.64, and 0.91 to 1.81 for the Singhora, the Chandarpur, and the Raipur Groups, respectively, whereas the topmost

Kharsiya Group has Gd_N/Yb_N of 1.21. The basement Bastar granitoids comprising the Dongargarh and Kanker granites, and the Baya Gneiss, show La_N/Yb_N in the range of 15.9 to 31.5 and Gd_N/Yb_N from 1.66 to 2.54, with conspicuous Nb, Ta, Sr, and Eu depletions and Th, U, and Pb enrichment, with respect to Primitive Mantle. Similarly, the single silty shale sample from the Arjuni Formation of the SGB exhibits La_N/Yb_N = 7.4 and Gd_N/Yb_N = 1.24 with Eu/Eu* = 0.64. The Sukhda Tuff displays enrichment in Pb and Th, whereas it shows prominent depletions in Nb, Ta, Sr, Zr, Hf, Eu, Ho, and Tm, when normalized to Primitive Mantle (Fig. 4.8 C). Overall, the tuff exhibits a highly enriched LREE pattern when normalized to Chondrite (Fig. 4.8 D), with La_N/Yb_N ranging from 86.4 to 103.4 and Gd_N/Yb_N from 17.5 to 20.9, respectively. The tuff also shows a prominent negative Eu anomaly with Eu/Eu* ranging from 0.45 to 0.70.

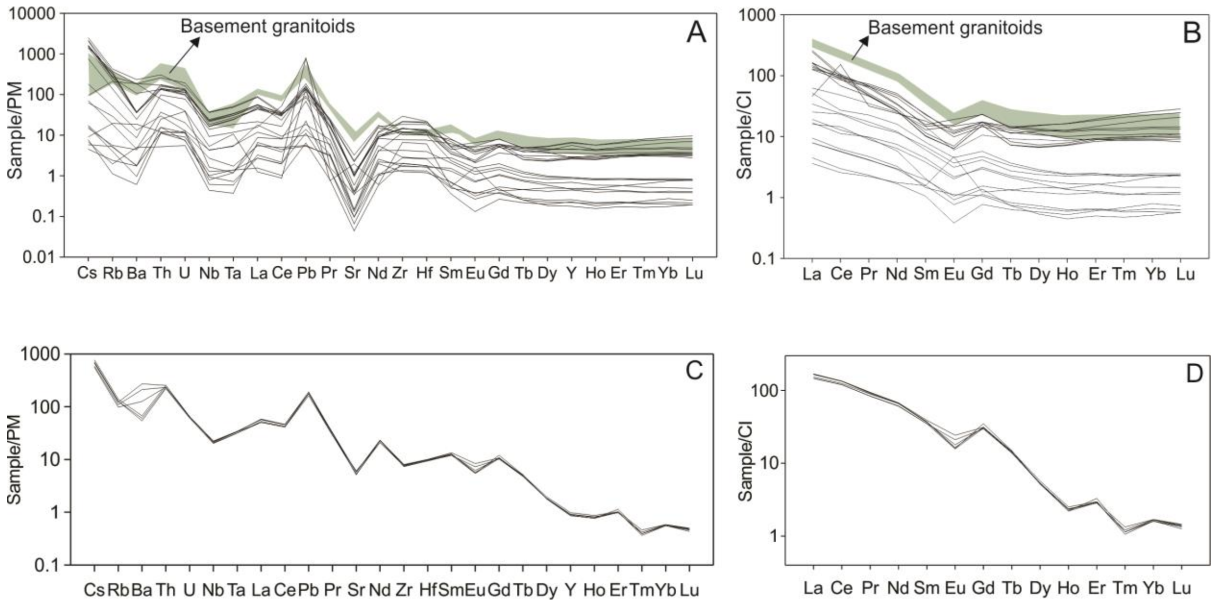

Figure 4.8: Primitive Mantle normalized multi-element (A) and Chondrite normalized rare earth element (REE) (B) patterns for siliciclastic samples from the Chhattisgarh Supergroup. Patterns for basement Bastar granitoids are given for comparison. Plots (C) and (D) show Primitive Mantle normalized multi-element and Chondrite normalized REE patterns, respectively, for Sukhda Tuff. The CI Chondrite and Primitive Mantle values are from Sun and McDonough, (1989).

4.5.4 Sr-Nd isotope geochemistry

The Chhattisgarh siliciclastics display $^{87}Sr/^{86}Sr$ in the range of 0.739848 to 1.13742 (Table 4.3). Since, $^{87}Sr/^{86}Sr$ ratios are often susceptible to alteration in Precambrian terrains largely due to the subsequent metamorphic events, and that the Supergroup is known to have undergone metamorphism, they have not been used here for interpretations. Sediments from the Chhattisgarh basin show a large variation in the $\varepsilon_{Nd}(0)$ ranging from -32.9 to -11.4 (Table 4.3). The Nd isotopic composition of the samples, when corrected for their approximate sedimentation ages [i.e., ε_{Nd} (T)], varies from -19.2 to -6.5, and -18.1 to -3.6, for the Singhora, and the Chandarpur Groups, respectively, whereas it has narrow range of values from -8.6 to -4.3 for the overlying fine-grained siliciclastics dominated Raipur Group. The ε_{Nd} (T) of the Nandeli shale from the topmost Kharsiya Group is -6.6. The basement rocks, which include the Dongargarh, and Kanker granites and the Baya Gneiss, show ε_{Nd} (0) of -37.1, -40.2, and -37.4, respectively. The silty shale sample from the Arjuni Formation of the SGB shows a ε_{Nd} (0) of -27.5. Chhattisgarh sediments display Depleted Mantle model ages (T_{DM}) from 1.8 to 3.4 Ga with a mode at 1.9 Ga (Table 4.3). The samples from the lower sequences, the Singhora and the Chandarpur Groups, have a T_{DM} in the range of 1.9 to 3.4 Ga with major peaks at 2.1 and 2.9 Ga, whereas the T_{DM} of the overlying Raipur Group display a narrow range of 1.8 to 2.5 Ga with mode at 1.9 Ga. The Kharsiya Group shale shows a T_{DM} of 1.9 Ga. Among the basement rocks, the Dongargarh Granite displays a T_{DM} of 3.2 Ga whereas both the Kanker Granite and the Baya Gneiss show a T_{DM} of 3.0 Ga. The silty shale sample of the Arjuni Formation shows a T_{DM} of 2.9 Ga. The Sukda tuff has $^{87}Sr/^{86}Sr$ in the range of 0.726388 to 0.732479, and ε_{Nd} (0) from -7.0 to -6.4, respectively. It also exhibits an average T_{DM} of ~2.1 Ga.

4.6 Discussion

4.6.1 Carbon isotope stratigraphy

The Charmuria and the Chandi limestones have $\delta^{13}C$ in the range of 2.6 to 3.6 ‰, and 3.2 to 3.6 ‰, respectively. There is a unidirectional increase in the $\delta^{13}C$ from bottom to the top of the formation in case of the Charmuria, whereas no particular trend is observed in the Chandi Limestone (Fig 4.9). The $\delta^{18}O$ of neither the Charmuria, nor the Chandi formations show any particular trend with values consistently range between -7.9 to -7.4‰, and -8.9 to -6.5‰, respectively. The $\delta^{13}C$ remains flat when plotted against $\delta^{18}O$ for the Charmuria Limestone, whereas it doesn't follow any particular trend in the Chandi Limestone (Figs. 4.6 D and 4.7 D). The enriched $\delta^{13}C$ values of both Charmuria and Chandi limestones are consistent with the late Mesoproterozoic (< 1.3 Ga) $\delta^{13}C$ values reported globally (Bartley and Kah, 2004). Based on $\delta^{13}C$ stratigraphy, a depositional age bracket of 1.3 Ga to 1.0 Ga can be argued for the formation with 1.0 Ga as the upper bound for the Supergroup.

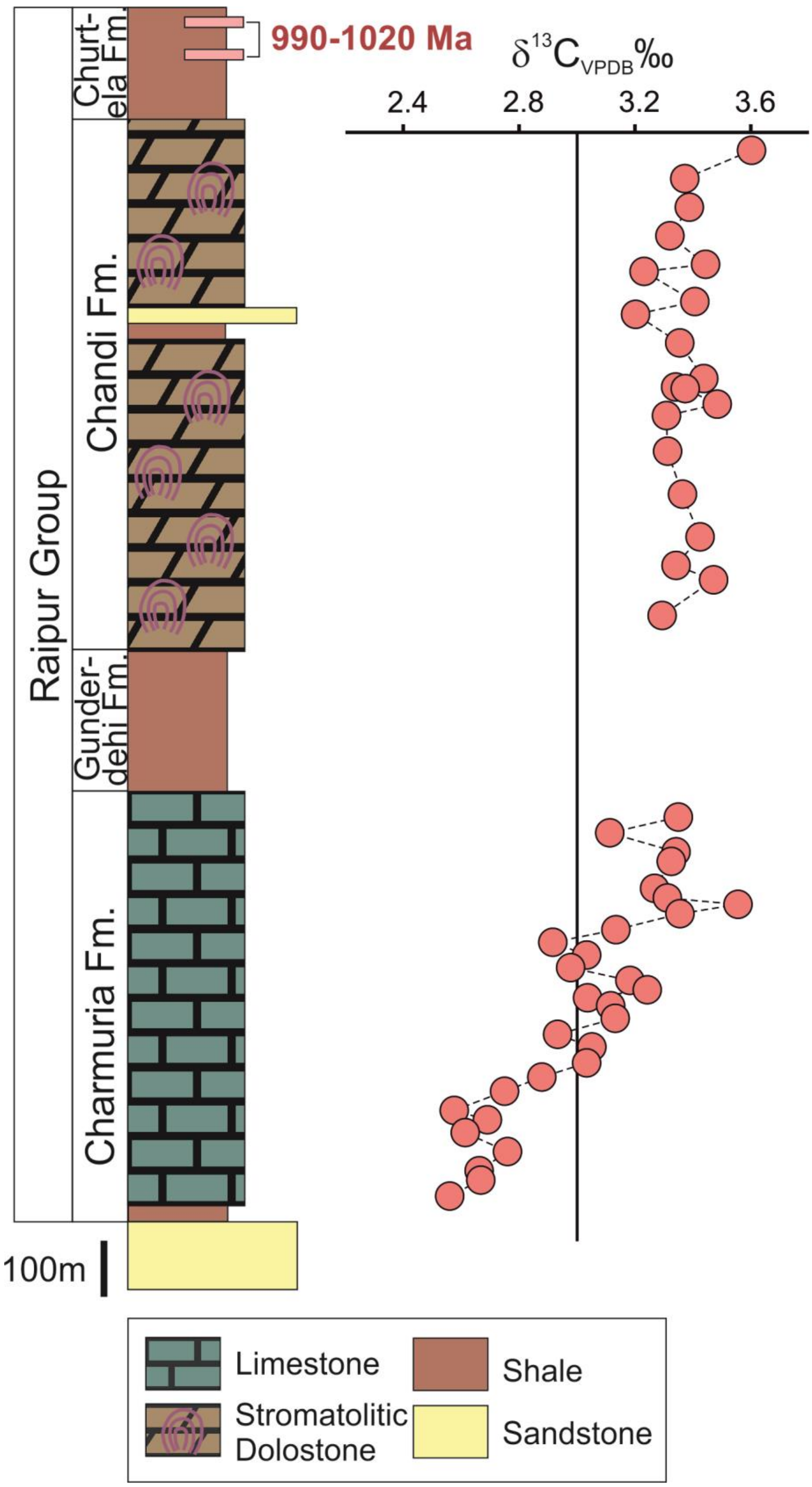

Figure 4. 9: Composite $\delta^{13}C$ stratigraphic profile for Charmuria and Chandi formations.

4.6.2 The Mesoproterozoic Ocean

The global carbon cycle is assumed to be in steady state equilibrium over geological time periods. The mantle carbon ($\delta^{13}C_{in}$ = ~ -5‰) entering the system is fractionated by the biology ($\delta^{13}C_{org}$) which preferentially takes up lighter carbon, leaving the contemporaneous marine carbonates ($\delta^{13}C_{carb}$) precipitated enriched (Des Marais et al., 1992; Kump and Arthur, 1999). Therefore, any observed shift in the $\delta^{13}C$ of the marine carbonates can be directly linked to the changes in the organic carbon burial flux (f_{org}) or, in short, primary productivity.

The sustained enriched $\delta^{13}C$ (2.6 – 3.6‰) displayed by the Raipur Group carbonates can be interpreted as a result of the increased organic carbon burial flux (f_{org}) during the late Mesoproterozoic, which succeeded a period of carbon isotope stasis in the Paleoproterozoic and early Mesoproterozoic when $\delta^{13}C$ of the marine carbonates remained close to 0‰ globally. However, the magnitude of the increase in the organic carbon burial flux (f_{org}) and the probable reasons that led to it are unclear. If we go by the conventional steady state notion, mass balance calculations suggest that it would take a 50% increase in the organic carbon burial flux (f_{org}) to prompt a +3.5‰ change in the $\delta^{13}C$ of the carbonate carbon, assuming that the $\delta^{13}C$ of the mantle carbon input and the biological fractionation ($\Delta = \delta^{13}C_{org} - \delta^{13}C_{carb}$) had remained similar to the present day values. The feasibility of sustaining such high organic carbon burial rates for a longer period of time however remains uncertain.

In the Chhattisgarh basin, there are sedimentary pyrites reported from within the Charmuria Limestone that show $\delta^{34}S$ ~ +25‰. Such ^{34}S enriched sulphides are produced by bacterial sulphate reduction (BSR) under closed system conditions in anoxic environments (Sarkar et al., 2010). The fact that these primary sedimentary pyrites were found along with the co-precipitating limestone indicates the existence of anoxic/euxinic conditions during the deposition of the Raipur Group. One of the ways this could happen is by an enhancement in the organic carbon burial (f_{org}) during the limestone deposition as discussed above. Similar anoxic conditions were also reported from both Vindhyan and Cuddappah basins during late Mesoproterozoic (Sarkar et al., 2010). Together, these arguments support our current understanding of the Mesoproterozoic Ocean; where the deep ocean remained largely anoxic while pockets of euxinia existed at the cratonic basin margins where biological productivity was high (Lyons et al., 2014).

Alternately, the increase in the $\delta^{13}C_{carb}$ could have been either by an increase in the $\delta^{13}C$ of the mantle carbon input ($\delta^{13}C_{in}$) or in the biological fractionation (Δ). An increase to the input carbon $\delta^{13}C$ to -1.5‰ or an increase in the biological fractionation to -42.5‰ could also yield +3.5‰ change in the $\delta^{13}C$ of the marine carbonates while keeping other parameters constant at the present day values. Nonetheless, the $\delta^{13}C_{org}$ values reported from the Proterozoic suggest biological fractionation remained similar to the present day values (Des Marais, 1994; Johnston et al., 2012). Additionally, there is no evidence yet to suggest any changes in the $\delta^{13}C$ of the mantle carbon input in the past.

Unlike the long term $\delta^{13}C_{carb}$ variations in the marine carbonates, the short term fluctuations in the $\delta^{13}C_{carb}$ are triggered by non-steady-state behaviour of the carbon cycle, which depends not only on the organic carbon burial flux (f_{org}) but also on the size of the dissolved carbon reservoir (approximated as DIC) (Kump and Arthur, 1999). A larger DIC reservoir acts as a buffer to the minor biogeochemical perturbations while its decreased size makes the $\delta^{13}C_{carb}$ more sensitive to biological changes. Therefore, the high $\delta^{13}C$ observed in the late Mesoproterozoic may not necessarily require a substantial increase in the f_{org}, but could have produced similar effect for a minor change in the f_{org}, if the carbon reservoir was sufficiently smaller.

4.6.3 Sediment provenance and basin evolution

The trace elemental patterns of the Chhattisgarh siliciclastics are similar to that of upper continental crust with typical Th, U and Pb enrichments and Nb, Ta, Sr and Eu depletions (Figs. 4.8 A and B). The total REE concentration is highly variable in the sandstone samples and the low total REE concentrations could be due to the dilution effect induced by quartz. All the samples show significant LREE enrichment (La_N/Yb_N = 1.7 to 37.3) suggesting influence of felsic sources throughout the sedimentation. The Singhora and the Chandarpur Groups show more felsic character with relatively flat HREE pattern and average Th/Sc of 1.0 to 5.8, whereas the Raipur and Kharsiya Groups siliciclastics show flat to enriched HREE pattern and Th/Sc ranging from 0.7 to 1.5, indicating a mixed provenance. Additionally, the Singhora and Chandarpur samples show minor degree of Zr enrichment away from the compositional variations possibly due to sediment recycling and exhibit large variation in the Th/Sc, and $f^{Sm/Nd}$ suggesting poor mixing and less transportation of the sediments (Fig. 4.10). The Raipur Group sediments and the Kharsiya Group shale fall along the compositional variations line in the Th/Sc vs. Zr/Sc plot (Fig. 4.10) and do not show any

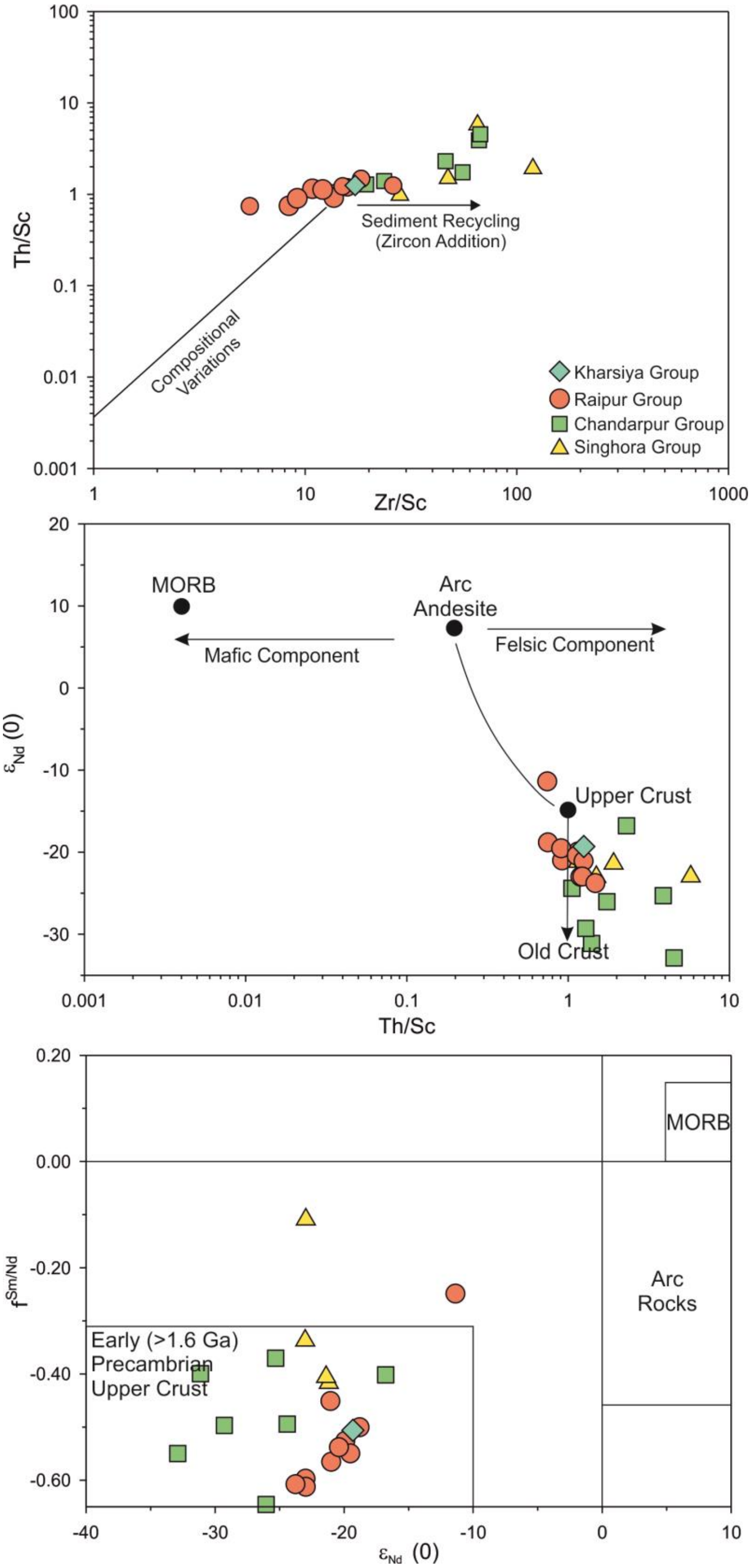

Figure 4.10: Plots of Th/Sc vs. Zr/Sc (A), ε_{Nd} (0) vs. Th/Sc (B) and $f^{Sm/Nd}$ vs. ε_{Nd} (0) (C) for samples from siliciclastic formations of the Chhattisgarh Supergroup.

evidence of sediment recycling and display an uniform Th/Sc, and f $^{Sm/Nd}$ indicating well mixed sediments.

The lower sequences, Singhora and Chandarpur, exhibit a large range of ε_{Nd} (t=1.2 Ga) from -20 to -4 whereas the sediments of the upper sequences, Raipur and Kharsiya, show ε_{Nd} (t=1.2 Ga) from -8 to -2 (Fig 4.11). Similarly, the T_{DM} of the Singhora and Chandarpur Groups varies from 1.8 to 3.4 Ga, and that of the fine-grained Raipur and Kharsiya sediments falls in a narrow range of 1.8 to 2.6 Ga. The mode of T_{DM} distribution falls at 1.9 Ga (Fig 4.12). This suggests that the Chhattisgarh sediments were derived from multiple sources of varying mantle derivation ages. The paleocurrent data from the basin suggests a NE-SW paleoflow during the deposition of both Singhora and Chandarpur groups (Bhattacharya and Patranabis-Deb, 2016; Chakraborty et al., 2015; Murti, 1987) with the exception of Bhalukona Formation which shows SE paleoflow direction (Chakraborty et al., 2012). We compared the REE and Nd isotopic data of Chhattisgarh Supergroup with that of the Archean and Paleoproterozoic lithounits located along the southwest and northern fringes, in an attempt to identify the potential sediment sources located within the vicinity of the basin. These included the basement Bastar granitoids: Dongargarh granites, Kanker granites and Baya gneisses, and the Sonakhan Greenstone Belt (SGB) in the south, the Sakoli, Nandagaon and Kairagarh Groups in the west, and the Mahakoshal Group, Tirodi Gneissic Complex (TGC), and the mafic granulites of RKG and BBG belts of the CITZ, located at the north and northwest of the basin.

The older T_{DM} (>2.2 Ga) and the less radiogenic ε_{Nd} (>-6) of the Chhattisgarh sediments could be attributed to the Archean and Paleoproterozoic basement granitoids of the Baster Craton in the south as well as the Paleoproterozoic Mahakoshal rocks in the northern margin of the basin. However, these granitic sources alone cannot explain the entire range of compositions shown by the Chhattisgarh sediments. The younger model ages and the relatively more radiogenic Nd isotopic compositions of the Chhattisgarh sediments can only be explained by a significant input of juvenile material into the basin. Although, the mafic volcanics of the SGB, the Sakoli, and the Kairagarh Groups could be probable sources of the higher ε_{Nd} (>-6) of the Chhattisgarh sediments, their older T_{DM} ages ($\geq$ 2.4 Ga) rule them out being the younger juvenile source/s. There are no Nd isotopic data available from the Nandagaon Group for comparison, nonetheless, they are considered older than the Kairagarh volcanics and could have contributed to the older provenance. Another probable younger sediment source is the Tirodi Gneissic Complex located in the Sausar Mobile Belt (SMB) which forms the western part of the CITZ. They are polygenetic in nature with the southern domain showing a Paleoarchean antiquity (T_{DM} c(Hf) = 3.1 – 3.6 Ga) and could have contributed to the older provenance (Bhowmik et al., 2011). The northern domain has a Paleoproterozoic antiquity (T_{DM} c(Hf) = 2.1 – 2.5 Ga; T_{DM} (Nd) = 2.1 – 2.5 Ga) and could have acted as the younger sediment sources (Ahmad et al., 2009; Bhowmik et al., 2011). Additionally, in the SMB, there are two mafic granulite belts, the RKG and the BBG, which are largely composed of tholeiitic gabbro with intercalated charnockite and could have supplied high radiogenic ε_{Nd} (<-6) to the basin; even though, they are limited in areal extent at present. The BBG belt, however, is of Neoarchean antiquity (T_{DM} c(Nd) = 2.4 - 2.5 Ga, ε_{Nd} (t=1.2 Ga) = -6.7 to -4.0) and could have contributed to the older provenance whereas the granulites of the RKG have a late Paleoproterozoic origin (T_{DM} c(Nd) = 1.9 - 2.0 Ga, ε_{Nd} (t=1.2 Ga) = -1.0 - -0.9) and fits the description of the younger provenance to the basin (Roy et al., 2006).

Since the REE's are generally resistant to weathering and post depositional alteration, we have utilized ε_{Nd} and La/Yb to quantify the contribution of sediments from the potential source rocks around Chhattisgarh basin. ε_{Nd} was corrected for the approximate age of sedimentation and La/Yb was chondrite-normalized. Three separate mixing curves were generated for Singhora, Chandarpur, Raipur and Kharsiya groups (Fig. 4.13). From the three component mixing diagrams, the following observations are made:

1) Sonakhan Greenstone Belt (SGB) was a major source of sediment (> 60%) for the Singhora and large part of the Chandarpur Group along with the basement Bastar Granitoids.

2) The later stage of Chandarpur sedimentation sees the provenance becoming more dominated by the Mahakoshal rocks (> 50%) and the mafic granulite belts, RKG and BBG, of the CITZ. This signifies a shift in provenance from the southern part of the basin towards the sources located in the north (Fig. 4.14). Overall, the sediment sources of the Chandarpur Group were diverse with the basement Baster Granitoids and Mahakoshal Group rocks contributed sediments equally along with the SGB with minor contributions from the mafic granulite belts.

3) By the time of deposition of the Raipur and Kharsiya Groups, the SGB and basement Bastar granitoids were largely cut-off as source regions. More than 90% of the

sediments were sourced from the northerly located mafic granulite belts and the Mahakoshal Group rocks with only minor inputs from the SGB (Fig. 4.15).

4) The bottommost Rehatikhol Sandstone falls outside the mixing curves due to its heterogeneous nature; however their Nd isotopic composition is identical to the Bastar granitoids attributing their origin to the basement.

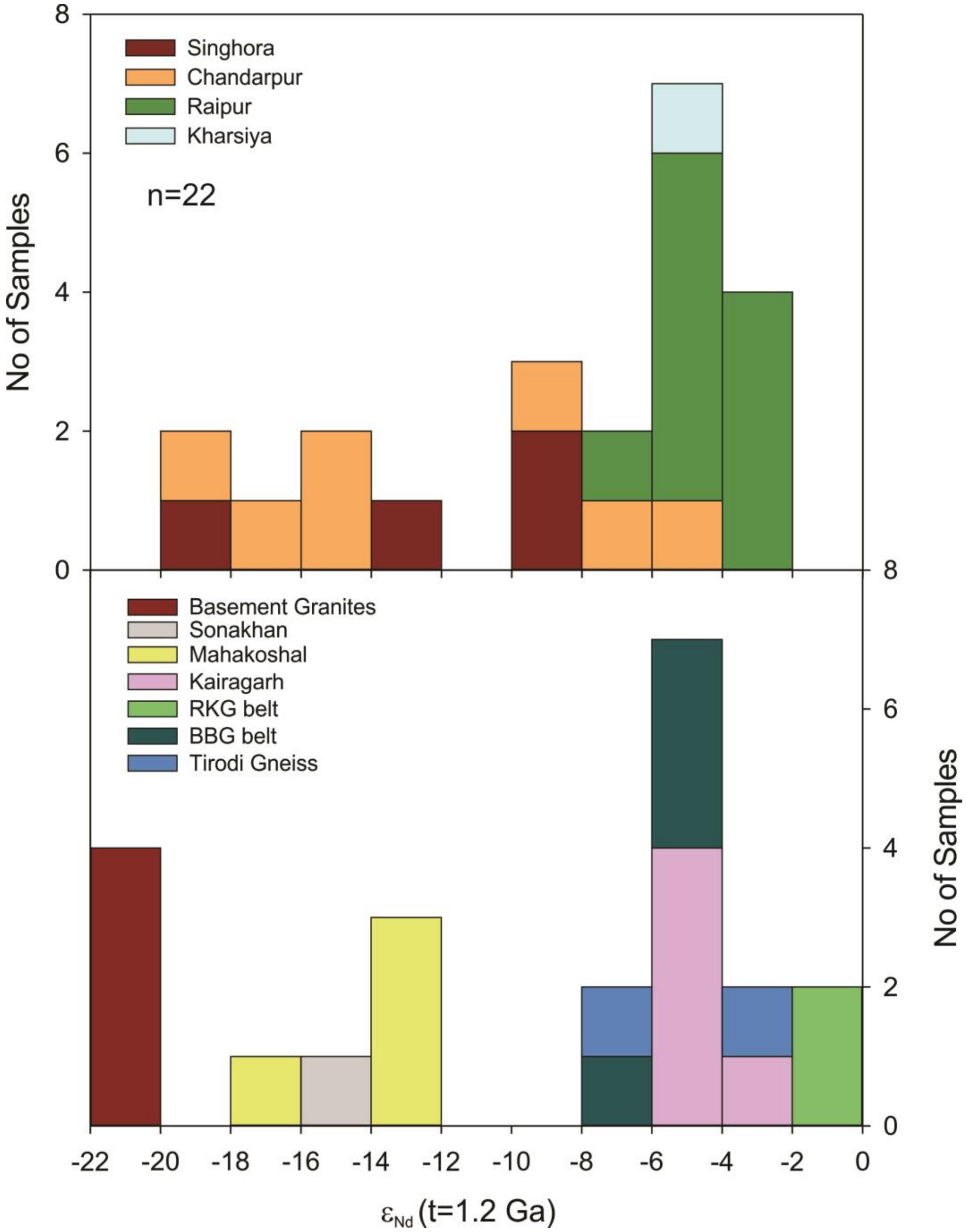

Figure 4.11: (A) Histogram of ε_{Nd} (t=1.2 Ga) distribution for the Chhattisgarh Supergroup (B) ε_{Nd} (t=1.2 Ga) distribution for the potential sources in a stacked histogram. Data for source rocks are from Ahmad et al., (2009); Bora et al., (2013); Bora and Kumar, (2015); Das et al., (2017); Longjam and Ahmad, (2012); Roy et al., (2006); Yadav et al., (2015) and this study (Table 4.3).

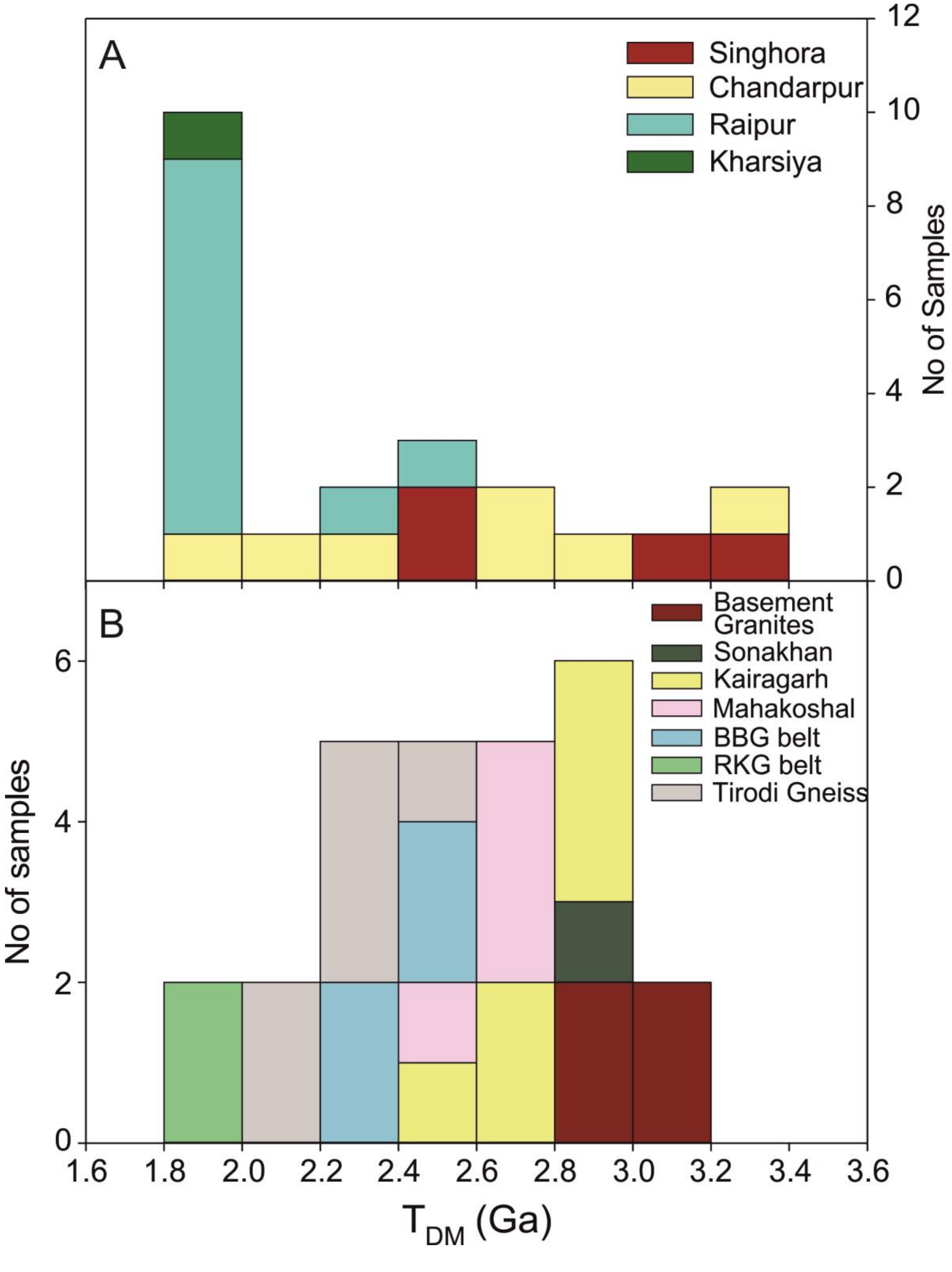

Figure 4.12: (A) Histogram of T_{DM} distribution for the Chhattisgarh Supergroup (B) Stacked histogram of T_{DM} distribution for the potential sources. Data sources as in Fig. 4.11.

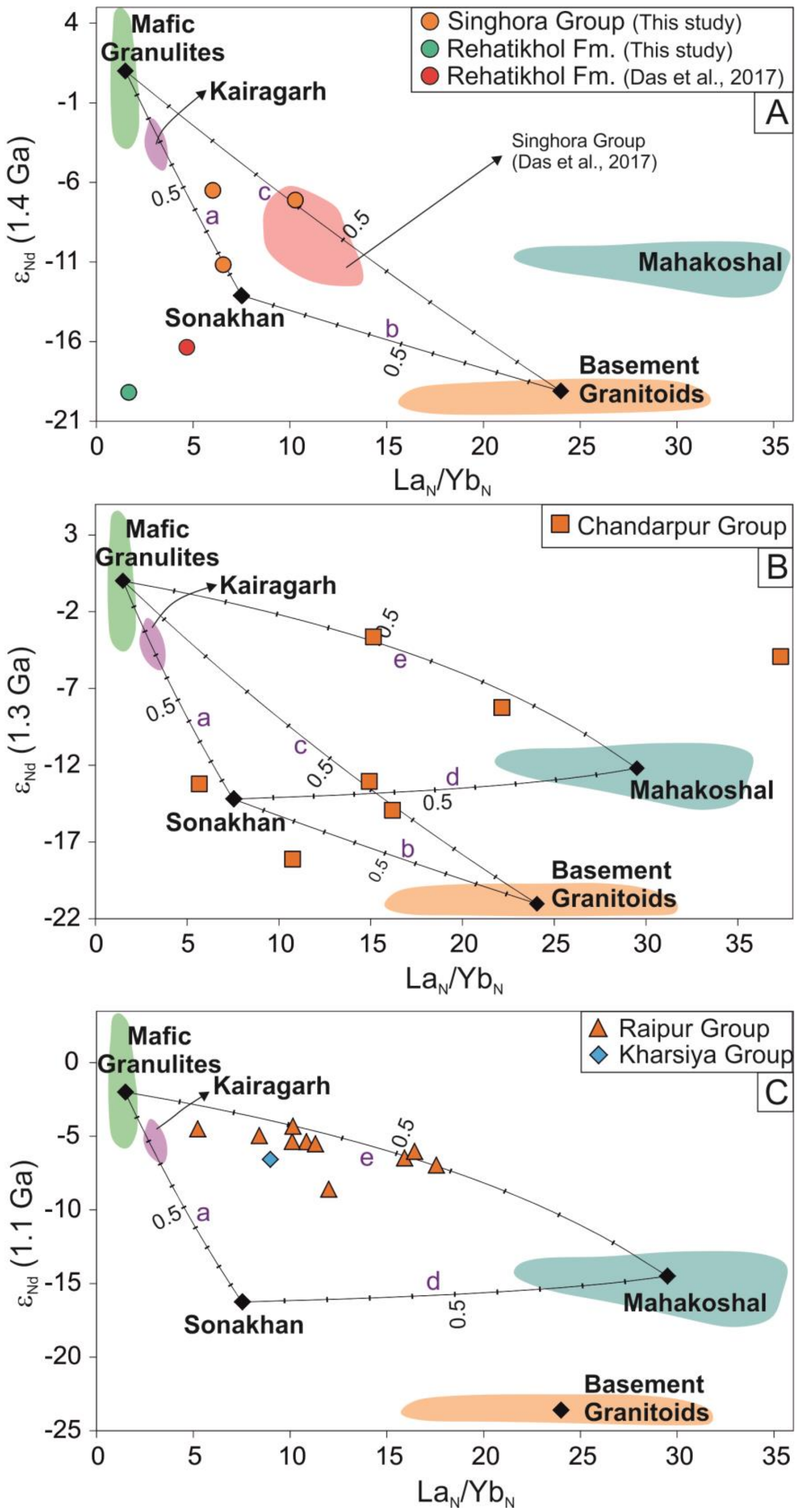

Figure 4.13: Plot of ε_{Nd} (T) vs. La_N/Yb_N for Chhattisgarh siliciclastics in the (A) Singhora Group, (B) Chandarpur Group, and (C) Raipur and Kharsiya Groups. Mixing curves are generated with mafic granulite belts of CITZ, Mahakoshal Group, Sonakhan Greenstone Belt and basement Bastar granitoids as end members. Mixing curves a, b, c, d, and e, are drawn for Nd/Yb ratios of 0.87, 0.94, 1.22, 2.40, and 0.50, respectively, for all the three plots. Data sources: as in Fig. 4.11.

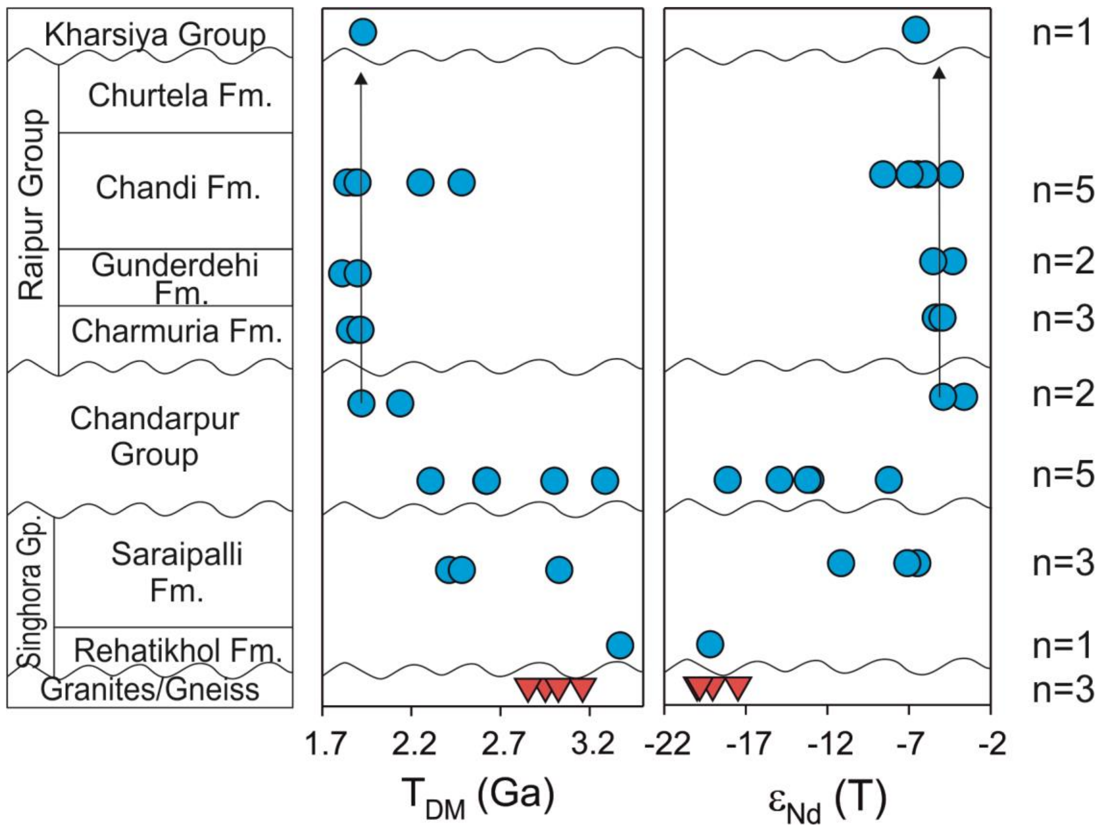

Figure 4.14: Variations of T_{DM} and ε_{Nd} (T) with stratigraphy in Chhattisgarh Supergroup.

4.6.4 On the origin of the Sukhda Tuff

The Sukhda Tuff shows enrichments in Pb and Th, and depletions in Nb, Ta, Sr, and Eu when plotted in a Primitive Mantle normalized multi-element diagram (Fig. 4.8 C and D). They also follow an LREE enriched pattern in a Chondrite normalized REE plot. These characteristics are typical of upper continental crust (UCC) and show the influence UCC in the parent magma. However, they also display conspicuous depletions in Ho and Tm and a steep depletion in the HREE pattern suggesting that garnet had remained in the residual phase during the partial melting of its source. The tuff shows an average $^{87}Sr/^{86}Sr$ of 0.702071 and ε_{Nd} of -6.6 (Fig. 4.16), when corrected for its crystallization age of ~1.0 Ga. The basement granitoids of the Baster Craton display $^{87}Sr/^{86}Sr$ (t=1.0 Ga) from 0.733428 to 0.802696 and ε_{Nd} (t=1.0 Ga) from -25.8 to -24.3. There are indications that the $^{87}Sr/^{86}Sr$ of the tuff and the basement were altered in the subsequent metamorphic events and the Sr isotope data should be viewed with caution. Nonetheless, the Nd isotopic ratios are quite robust and the ε_{Nd} (t=1.0 Ga) of the Sukhda Tuff is quite different from that of the basement Baster granitoids ruling out the possibility of them being the result of partial melting of the basement. Their relatively high radiogenic ε_{Nd} (0) suggest their derivation from a deeper mafic source. However, the tuff

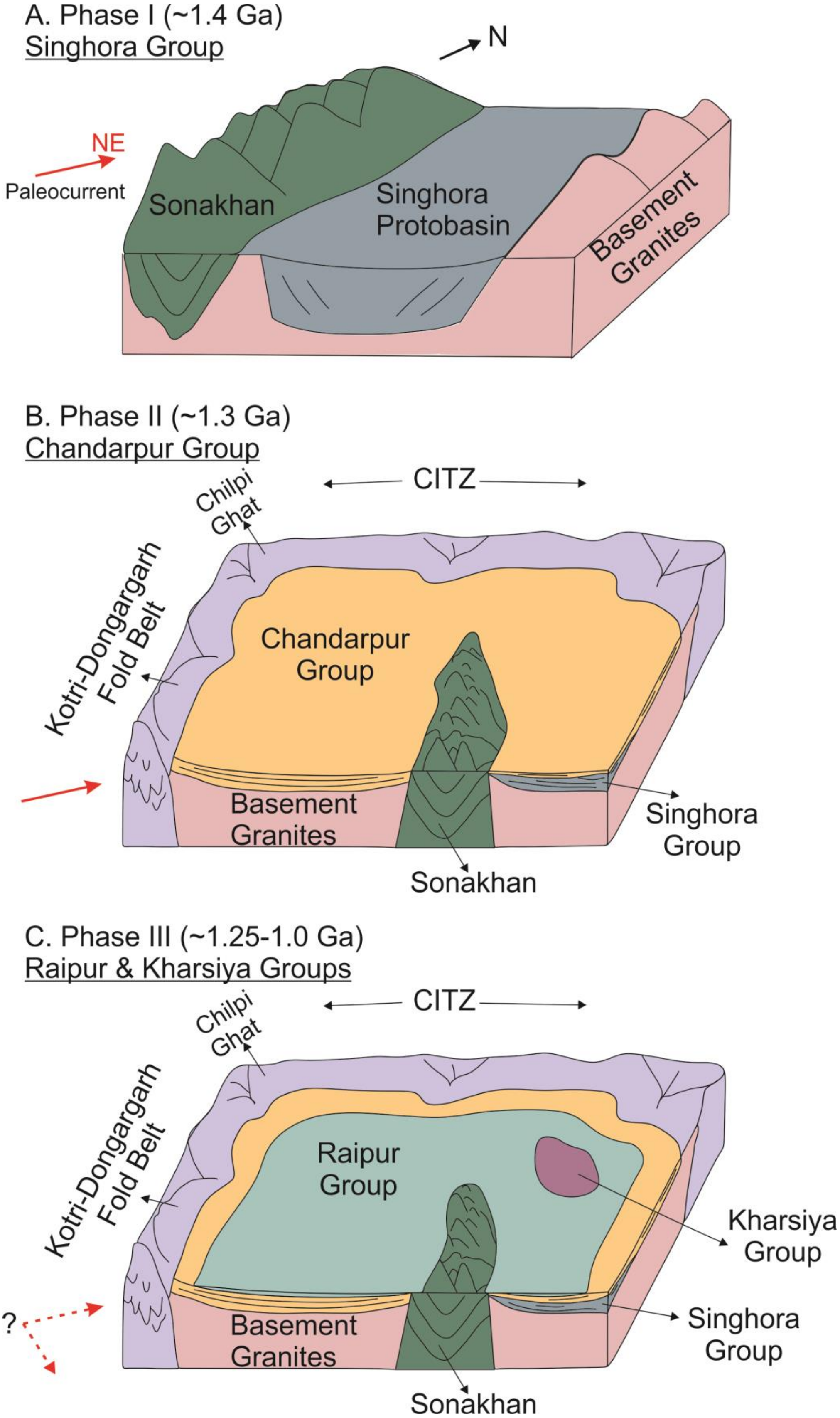

Figure 4.15: Proposed model for the evolution of the Chhattisgarh Basin in three phases (modified after Das et al., 1992). See text for discussion.

displays a T_{DM} of 2.1 Ga, significantly older than its crystallization age, but younger than the T_{DM} of most of the basement rocks of the Bastar Craton along with relatively less radiogenic ε_{Nd} (t=1.0 Ga) compared to that of the average juvenile mafic sources. This suggests that the Sukhda Tuff could have been derived from the partial melting of a mafic source, but had assimilated significant amount of Archean or early Paleoproterozoic continental crust likely from the basement Baster Granitoids, either during its evolution or during its ascent at ~1.0 Ga.

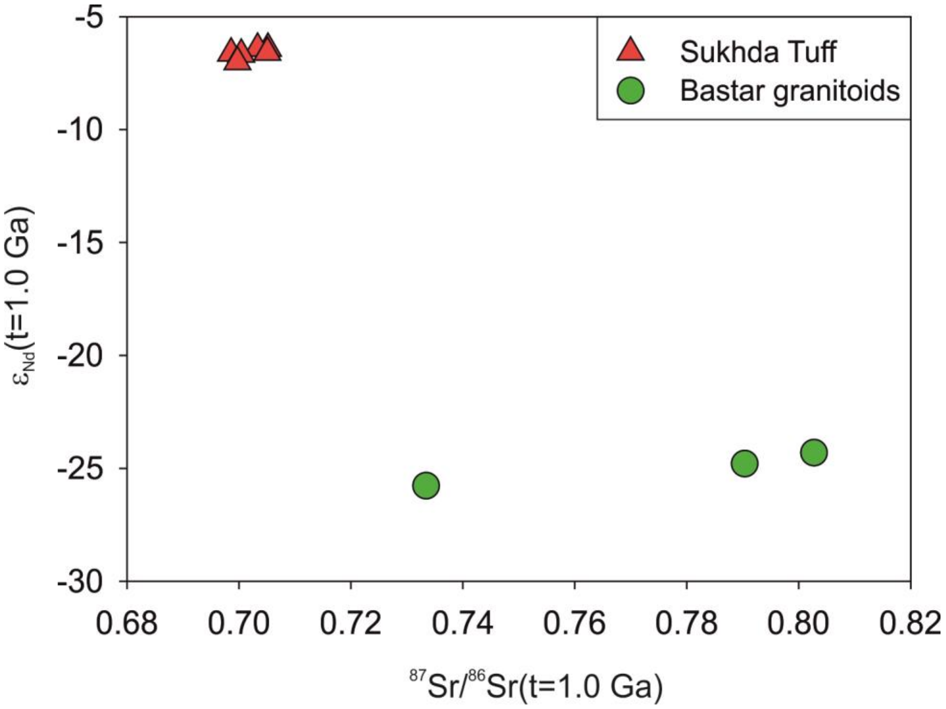

Figure 4.16: Plot of ε_{Nd} (t=1.0 Ga) versus $^{87}Sr/^{86}Sr$ (t=1.0 Ga) of Sukhda Tuff.

4.6.5 On the timing of the amalgamation of the Indian cratons/blocks

The South Indian Block (SIB), comprising Dharwar and Baster cratons was amalgamated with the North Indian Block (NIB) consisting of the Bundelkhand Craton, forming the unified Indian landmass sometime during the late Paleoproterozoic to early Neoproterozoic. The rocks of the CITZ are believed to have recorded the history of this continent-continent collision. The timing of this suture, however, remains equivocal. Some argue in favour of an ~1.6 Ga age for this event (Dey et al., 2017; Meert et al., 2010; Meert and Santosh, 2017), whereas others suggest that the amalgamation occurred at ~1.0 Ga during the Grenvillean Orogeny (Bhowmik et al., 2012; Bickford et al., 2011b; Roy et al., 2006). There are also suggestions of a two-stage accretion event with closure of oceanic basins at both ~1.55 and at ~1.0 Ga (Rekha et al., 2011). All three arguments are supported by the ubiquitous ~1.6 Ga and ~1.0 Ga magmatic zircons and monazites (U-Pb ages) in the rocks of CITZ. The Chhattisgarh basin is developed at the northern fringe of the SIB and is largely surrounded by rocks of Archean and early Paleoproterozoic antiquity, except in the northern part where it is bound by the CITZ. The distribution of the rocks in various crustal domains of the CITZ follows a trend. The southern sector of each crustal domain have an Archean antiquity, whereas the northern sectors are generally of late Paleoproterozoic age (Bhowmik et al., 2011; Roy et al., 2006). The T_{DM} as well as the quantitative provenance analysis of the Chhattisgarh siliciclastics has shown that a significant portion of the sediments, mainly of the Raipur and Kharsiya Groups, is of late Paleoproterozoic antiquity. This implies two things: 1) The Paleoproterozoic provenance of the upper Chhattisgarh rocks is derived from the CITZ as discussed in the section 4.6.3, and it would mean that the amalgamation of NIB and SIB might have happened at ~1.6 Ga, much before the initiation of sedimentation in the Chhattisgarh basin at ~1.45 Ga. 2) Alternatively, there were other Paleoproterozoic sources in the northern fringes of the SIB which had supplied sediments during the evolution of the Chhattisgarh basin, but got obliterated during the amalgamation of NIB and SIB at the beginning of Neoproterozoic at ~1.0 Ga. The first scenario appears more plausible. This suggests that the peninsular India had almost attained its present day configuration by the time of maximum packing of the Columbia Supercontinent at ~1.45 Ga (Meert and Santosh, 2017) and can be considered as a single landmass for the continental reconstructions beyond the Rodinia.

4.7 Conclusions

From our geochemical study of rocks of the Chhattisgarh Supergroup we conclude the following.

1. The $\delta^{13}C$ stratigraphy along with the available age constraints from the basin places the age of formation of the Raipur Group between 1.3 and 1.0 Ga.

2. The presence of ^{13}C enriched carbon in the Raipur carbonates ($\delta^{13}C$ = 2.6 to 3.6 ‰) suggests an increase in the organic carbon burial fluxes during Mesoproterozoic. Our data support the view that the deep ocean remained anoxic; whereas euxinia existed in the cratonic basin margins where organic carbon burial fluxes were high.

3. The quantitative provenance analysis of the Chhattisgarh siliciclastics revealed that the lower Chhattisgarh sediments were largely supplied by the Sonakhan Greenstone Belt and the

basement Bastar granitoids, whereas the upper Chhattisgarh formations were contributed by the mafic granulite belts and Mahakoshal rocks of the CITZ.

4. The provenance analysis has also revealed that the basin received substantial detritus from the younger Paleoproterozoic sources located at the CITZ in the north, which in turn suggests that the amalgamation of NIB and SIB had already taken place at ~1.6 Ga, much before the initiation of sedimentation in the Chhattisgarh basin.

5. Trace element and Sr-Nd isotopic study of the Sukhda Tuff attributes its origin to the partial melting of a mafic source. The tuff had assimilated significant amount of Archean or early Paleoproterozoic continental crust, likely from the basement Bastar granitoids, during its evolution.

Table 4.1: Details of samples from Chhattisgarh Supergroup and adjacent basement rocks.

Sample ID	Formation/Group	Location	Description
Chhattisgarh Supergroup			
CH 15-103	Singhora	N 21.275; E 83.087	Shale
CH 15-104	Singhora	N 21.275; E 83.087	Medium-grained sandstone (quartz-arenite)
CH 15-105	Singhora	N 21.274; E 83.086	Fine-grained sandstone (quartz-arenite)
CH 15-106	Singhora	N 21.312; E 83.230	Feldspathic arenite
CH 15-76	Chandarpur	N 21.078; E 80.835	Medium-grained red sandstone (quartz arenite)
CH 15-78	Chandarpur	N 21.099; E 80.845	Medium-grained red sandstone (quartz arenite)
CH 15-79	Chandarpur	N 21.099; E 80.845	Medium-grained grey sandstone (quartz arenite)
CH 15-84	Chandarpur	N 21.178; E 82.045	Silty sandstone
CH 15-96	Chandarpur	N 21.541; E 82.510	Silty sandstone
CH 15-102	Chandarpur	N 21.583; E 83.116	Quartz arenite
CH 15-99	Chandarpur	N 21.940; E 83.343	Quartz arenite
CH S-1,2,3	Charmuria	N 21.039; E 80.944	Shale/Mud
CH 15 47-75	Charmuria	N 21.039; E 80.944	Limestone
CH 15-97	Gunderdehi	N 21.662; E 82.741	Calcareous shale
CH 15-98	Gunderdehi	N 21.620; E 82.969	Stromatolitic calcareous shale
CH 15-44	Chandi	N 21.190; E 81.217	Sandstone
CH 15-45	Chandi	N 21.190; E 81.217	Sandy shale
CH 15-21	Chandi	N 21.852; E 81.156	Stromatolitic dolostone
CH 15-32	Chandi	N 21.852; E 81.156	Stromatolitic dolostone
CH 15-40	Chandi	N 21.852; E 81.156	Stromatolitic dolostone
CH 15 21-40	Chandi	N 21.852; E 81.156	Stromatolitic dolostone
CH 15-100	Kharsiya	N 21.985; E 83.210	Calcareous shale
CH 15-101A-F	Sukhda Tuff	N 21.867; E 83.097	Felsic tuff
Basement rocks			
CH 15-85	Kanker	N 21.216; E 82.239	Granite
CH 15-88	Baya	N 21.310; E 82.532	Granite gneiss
CH 15-09	Dongargarh	N 21.077; E 80.325	Granite
CH 15-95	Sonakhan	N 21.541; E 82.521	Silty shale (Arjuni Fm.)

Note: Locations are given in degree

Table 4.2: Geochemical data of carbonate formations of the Chhattisgarh Supergroup.

Sample ID	$\delta^{13}C_{VPDB}$(‰)	$\delta^{18}O_{VPDB}$ (‰)	Depth (m)	Mg/Ca	Ca/Sr	Mn/Sr	$^{87}Sr/^{86}Sr$
Charmuria Formation							
15-47	3.4	-7.9	0	0.03	1309	2.6	0.70742
15-48	3.1	-7.8	0.5				
15-49	3.3	-7.7	1.1	0.03	1087	2.1	
15-50	3.3	-7.7	1.4	0.03	1358	2.4	0.70766
15-51	3.3	-7.7	2.25				
15-52	3.3	-7.6	2.55				
15-53	3.6	-7.6	2.75	0.03	1386	2.7	0.70775
15-54	3.4	-7.5	3.05				
15-55	3.1	-7.6	3.55	0.03	1381	3.4	
15-56	2.9	-7.7	3.95	0.04	1115	2.7	0.70861
15-57	3.0	-7.7	4.35	0.02	1224	2.9	
15-58	3.0	-7.7	4.75				
15-59	3.2	-7.4	5.15	0.04	891	1.9	0.70734

Sample ID	$\delta^{13}C_{VPDB}$(‰)	$\delta^{18}O_{VPDB}$ (‰)	Depth (m)	Mg/Ca	Ca/Sr	Mn/Sr	$^{87}Sr/^{86}Sr$
15-60	3.2	-7.6	5.45	0.03	1035	2.4	0.70725
15-61	3.0	-7.7	5.7				
15-62	3.1	-7.6	5.95	0.03	971	2.7	
15-63	3.1	-7.8	6.35				
15-64	2.9	-7.7	6.85	0.03	1288	2.8	0.70802
15-65	3.1	-7.6	7.25				
15-66	3.0	-7.6	7.75	0.03	793	2.0	0.70723
15-67	2.9	-7.7	8.2	0.04	507	1.2	
15-68	2.7	-7.6	8.65				
15-69	2.6	-7.8	9.25	0.04	1027	2.8	0.70782
15-70	2.7	-7.7	9.55				
15-71	2.6	-7.9	9.95	0.07	653	2.0	0.70785
15-72	2.8	-7.8	10.55				
15-73	2.7	-7.8	11.15	0.03	1016	2.9	
15-74	2.7	-7.7	11.45				
15-75	2.6	-7.8	11.95	0.05	821	2.7	0.70814
Chandi Formation							
15-21	3.6	-6.5	0	0.08	1660	3.2	0.71047
15-22	3.4	-8.6	0.2	0.04	1783	2.8	0.70978
15-23	3.4	-8.7	0.4				
15-24	3.3	-8.8	0.6				
15-25	3.4	-8.6	0.8	0.05	1586	2.3	0.70953
15-26	3.2	-8.2	0.85	0.06	1730	2.4	
15-27	3.4	-8.5	1.06				
15-28	3.2	-8.8	1.15	0.06	1492	1.8	0.70962
15-29	3.4	-8.8	1.35				
15-30	3.4	-7.8	1.6	0.43	744	2.7	0.71371
15-31	3.3	-8.5	1.66				
15-32	3.4	-8.8	1.67				
15-33	3.5	-8.5	1.78	0.05	1611	2.7	0.70816
15-34	3.3	-8.7	1.86	0.07	934	1.8	
15-35	3.3	-8.8	2.11				
15-36	3.4	-8.8	2.41	0.05	1496	2.7	0.71065
15-37	3.4	-8.6	2.71				
15-38	3.3	-8.9	2.91	0.05	1490	2.0	
15-39	3.5	-8.5	3.01	0.06	1571	2.5	
15-40	3.3	-8.9	3.26	0.26	598	1.6	0.71250

Note: Concentrations were measured using Q-ICPMS. External reproducibility for Ca and other trace elements were <6% at 2σ level.

Table 4.3: Geochemical data for samples from siliciclastic and volcanicalstic formations, and silicate fractions in limestones of the Chhattisgarh Supergroup.

	Singhora Group				Chandarpur Group		
Sample ID	CH 15-103	CH 15-104	CH 15-105	CH 15-106	CH 15-76	CH 15-78	CH 15-79
Sc	8.5	1.10	0.65	1.14	0.94	2.43	2.39
V	24	4.3	5.2	6.1	6.2	10.8	14
Cr	71	93	173	93	204	193	200
Co	2.8	0.27	0.21	0.14	0.18	0.99	0.38
Ni	11.1	0.46	1.07	0.83	1.4	5.5	3.1
Rb	19	3.3	1.5	133	3.6	11.7	33
Sr	12.2	8.2	2.0	41	2.8	3.1	7.1
Y	13.4	4.1	2.0	2.2	3.1	3.9	4.1
Zr	238	131	31	75	22	47	32
Nb	9.9	1.17	0.67	3.8	1.9	3.0	3.1
Cs	0.50	0.046	0.036	0.75	0.12	0.56	1.4
Ba	60	12.2	12.2	1281	31	32	92
La	14.8	6.0	1.88	0.86	3.8	8.1	12.2
Ce	29.3	14.3	3.4	1.57	8.8	14.6	16.6
Pr	3.31	1.45	0.39	0.210	0.85	1.65	2.14
Nd	11.7	5.4	1.39	0.82	2.97	5.6	7.5
Sm	2.22	1.05	0.300	0.239	0.583	0.923	1.23
Eu	0.35	0.213	0.061	0.272	0.117	0.182	0.263
Gd	2.18	0.97	0.32	0.25	0.64	0.85	1.18
Tb	0.34	0.123	0.049	0.050	0.084	0.101	0.136
Dy	2.25	0.68	0.307	0.37	0.49	0.60	0.73
Ho	0.48	0.136	0.064	0.081	0.097	0.128	0.139
Er	1.54	0.41	0.199	0.272	0.276	0.39	0.41
Tm	0.247	0.062	0.029	0.047	0.038	0.058	0.059
Yb	1.76	0.42	0.205	0.37	0.251	0.39	0.40
Lu	0.273	0.061	0.030	0.058	0.036	0.059	0.057
Hf	6.2	3.1	0.80	1.9	0.54	1.22	0.83
Ta	0.75	0.049	0.029	0.43	0.070	0.22	0.22
Pb	11.1	4.8	1.6	10.0	0.40	0.71	1.3
Th	8.3	2.1	0.98	6.6	1.32	3.1	2.5
U	1.6	0.80	0.26	0.83	0.24	0.43	0.27
Th/Sc	1.0	1.9	1.5	5.8	1.4	1.3	1.1
Zr/Sc	28	119	47	65	24	19	13
La_N/Yb_N	6.0	10.3	6.6	1.7	10.7	14.9	22.1
Gd_N/Yb_N	1.0	1.9	1.3	0.6	2.1	1.8	2.5
Eu/Eu*	0.48	0.65	0.60	3.38	0.58	0.63	0.67
$^{87}Sr/^{86}Sr$	0.807665	0.763870	0.769672	0.889426	0.839412	0.922098	0.923913
$^{143}Nd/^{144}Nd$	0.511552	0.511541	0.511458	0.511461	0.511042	0.511137	0.511387
ε_{Nd} (0)	-21.2	-21.4	-23.0	-23.0	-31.1	-29.3	-24.4
T_{DM} (Ga)	2.4	2.5	3.0		3.3	2.6	2.3

	Chandarpur Group				Raipur Group		
Sample ID	CH 15-84	CH 15-96	CH 15-102	CH 15-99	CH S-1	CH S-2	CH S-3
Sc	0.34	0.41	0.23	0.25	23	24	19
V	2.40	3.6	2.2	2.1	134	130	108
Cr	129	171	120	116	96	95	60
Co	0.27	0.16	0.14	0.08	5.7	4.9	8.6
Ni	1.5	1.12	0.49	0.26	17.2	10.7	29
Rb	2.5	3.2	12.3	1.2	270	236	175
Sr	0.93	3.2	7.4	2.0	22	20	25
Y	1.03	2.1	1.00	0.81	31	29	26
Zr	23	19	15	14	243	328	161
Nb	0.72	0.57	0.43	0.31	26	26	16
Cs	0.13	0.14	0.071	0.054	20	17	13
Ba	6.7	13	130	35	1634	1280	1316
La	1.06	4.0	2.25	4.5	58	61	38
Ce	1.81	6.8	3.8	7.8	60	65	42
Pr	0.221	0.93	0.44	0.90	6.0	6.3	4.4
Nd	0.78	3.5	1.51	2.70	15.5	16.1	12.1
Sm	0.161	0.68	0.222	0.313	2.40	2.28	1.98
Eu	0.022	0.126	0.065	0.053	1.10	0.89	0.86
Gd	0.16	0.61	0.220	0.283	4.7	4.8	3.6
Tb	0.024	0.079	0.028	0.027	0.53	0.51	0.42
Dy	0.15	0.43	0.167	0.136	3.9	3.8	3.10
Ho	0.030	0.076	0.034	0.025	0.92	0.94	0.72
Er	0.100	0.210	0.106	0.083	3.05	3.19	2.42
Tm	0.018	0.030	0.015	0.012	0.54	0.59	0.43
Yb	0.135	0.190	0.100	0.087	3.9	4.4	3.24
Lu	0.018	0.028	0.014	0.014	0.62	0.71	0.52
Hf	0.55	0.51	0.41	0.37	6.5	6.8	4.3
Ta	0.057	0.049	0.024	0.015	2.0	2.1	1.25
Pb	0.46	0.98	57	0.38	6.4	9.4	10.1
Th	1.33	0.95	1.02	0.44	26	22	14
U	0.15	0.16	0.24	0.12	3.4	4.0	2.7
Th/Sc	3.9	2.3	4.5	1.7	1.1	0.9	0.7
Zr/Sc	66	46	67	55	11	14	8
La_N/Yb_N	5.7	15.1	16.2	37.3	10.8	10.1	8.4
Gd_N/Yb_N	1.0	2.6	1.8	2.7	1.0	0.9	0.9
Eu/Eu*	0.42	0.60	0.90	0.55	1.00	0.83	0.99
$^{87}Sr/^{86}Sr$	0.831690	0.769795	0.831616	0.739848	1.137420		0.952471
$^{143}Nd/^{144}Nd$	0.511341	0.511778	0.510952	0.511303	0.511617	0.511561	0.511674
ε_{Nd} (0)	-25.3	-16.8	-32.9	-26.0	-19.9	-21.0	-18.8
T_{DM} (Ga)	3.0	2.1	2.6	1.9	1.9	1.9	1.9

	Raipur Group						
Sample ID	CH 15-97	CH 15-98	CH 15-44	CH 15-45	CH 15-21*	CH 15-32*	CH 15-40*
Sc	13	10.8	0.76	16	10.2	9.1	9.1
V	78	75	11.0	203	106	86	93
Cr	71	64	213	271	94	73	89
Co	17	11.8	0.80	23	20	13	13
Ni	41	27	2.0	28	43	32	29
Rb	163	143	0.71	88	232	201	208
Sr	68	46	1.4	8.7	22	22	21
Y	21	16	1.17	13	13	11.8	12.3
Zr	115	130	20	86	161	137	167
Nb	11.5	11.9	0.90	6.6	17	15	16
Cs	12.5	11.0	0.061	6.0	11.3	12.2	13
Ba	747	249	4.2	172	256	249	262
La	32.7	29.8	1.86	10.8	38	34	39
Ce	56	52	3.5	93	63	54	58
Pr	6.9	6.3	0.40	3.01	4.8	4.4	4.6
Nd	23.6	20.3	1.35	11.2	13.3	12.2	12.3
Sm	3.5	3.06	0.24	2.74	1.76	1.55	1.57
Eu	0.73	0.57	0.044	0.64	0.40	0.37	0.37
Gd	3.5	2.99	0.233	3.24	3.6	3.17	3.14
Tb	0.50	0.43	0.030	0.47	0.304	0.267	0.269
Dy	3.25	2.68	0.185	2.81	1.85	1.67	1.72
Ho	0.68	0.57	0.036	0.52	0.45	0.41	0.42
Er	2.12	1.78	0.108	1.48	1.54	1.38	1.46
Tm	0.327	0.28	0.016	0.225	0.256	0.229	0.239
Yb	2.31	1.89	0.111	1.48	1.69	1.50	1.59
Lu	0.33	0.274	0.016	0.205	0.251	0.228	0.242
Hf	3.2	3.6	0.50	2.3	4.0	3.5	3.8
Ta	0.98	1.01	0.056	0.48	1.4	1.3	1.4
Pb	9.5	11.2	0.79	55	11.4	8.2	5.9
Th	11.3	12.1	0.95	11.6	12.1	11.2	13
U	2.0	2.1	0.19	2.6	2.4	2.3	2.7
Th/Sc	0.9	1.1	1.2	0.7	1.2	1.2	1.5
Zr/Sc	9	12	26	5	16	15	18
La_N/Yb_N	10.1	11.3	12.0	5.2	15.9	16.4	17.6
Gd_N/Yb_N	1.2	1.3	1.7	1.8	1.8	1.7	1.6
Eu/Eu*	0.64	0.58	0.57	0.66	0.49	0.51	0.51
$^{87}Sr/^{86}Sr$	0.798180	0.825518		1.015884			
$^{143}Nd/^{144}Nd$	0.511637	0.511592	0.511558	0.512055	0.511459	0.511460	0.511419
ε_{Nd} (0)	-19.5	-20.4	-21.1	-11.4	-23.0	-23.0	-23.8
T_{DM} (Ga)	1.8	1.9	2.3	2.5	1.9	1.8	1.9

	Kharsiya Group	Kanker Granite	Baya Gneiss	Dongargarh Granite	Sonakhan (Arjuni)	Sukhda Tuff	
Sample ID	CH 15-100	CH 15-85	CH 15-88	CH 15-09	CH 15-95	CH 15-101A	CH 15-101B
Sc	11.9	9.9	4.2	5.2	4.5	1.17	1.24
V	81	25	11.8	11.6	21	3.8	3.9
Cr	78	165	156	154	103	65	54
Co	6.9	5.3	2.3	3.0	1.3	1.8	2.1
Ni	15	6.2	3.6	5.3	2.8	1.5	2.1
Rb	170	118	231	233	90	69	77
Sr	49	243	133	143	16	129	124
Y	20.4	16	41	30	13	4.2	4.4
Zr	205	117	134	128	206	83	90
Nb	13	13	26	25	7.5	15	16
Cs	16	0.69	0.67	8.4	3.6	4.7	5.2
Ba	250	1302	1064	653	360	1474	1900
La	30.4	70	95	69	14.8	35	40
Ce	61	119	169	122	27.5	73	82
Pr	6.5	11.7	16.6	12.5	3.13	7.9	8.9
Nd	22.1	37	53	41	11.0	28.4	31.5
Sm	3.6	5.2	8.2	6.7	2.12	5.3	5.9
Eu	0.67	1.42	1.14	0.93	0.43	1.22	1.40
Gd	3.6	4.9	8.2	6.4	2.10	6.1	6.4
Tb	0.54	0.53	1.04	0.86	0.311	0.52	0.55
Dy	3.4	2.68	6.1	4.9	2.02	1.36	1.45
Ho	0.71	0.53	1.26	0.98	0.41	0.134	0.142
Er	2.24	1.54	3.87	2.97	1.27	0.47	0.49
Tm	0.355	0.224	0.59	0.45	0.201	0.031	0.034
Yb	2.43	1.59	4.1	3.10	1.40	0.287	0.288
Lu	0.361	0.256	0.60	0.45	0.213	0.036	0.037
Hf	5.6	2.9	3.6	4.2	5.1	2.9	3.1
Ta	1.11	0.60	2.5	2.3	0.60	1.30	1.38
Pb	13	20	39	26	4.7	11.5	13
Th	15	20	51	35	8.6	20	22
U	2.9	2.9	4.1	9.4	0.90	1.36	1.35
Th/Sc	1.3	2.0	12.0	6.7	1.9	17	17
Zr/Sc	17	12	32	25	46	71	73
La_N/Yb_N	9.0	31.5	16.7	15.9	7.54	86	100
Gd_N/Yb_N	1.2	2.5	1.7	1.7	1.2	17.5	18.3
Eu/Eu*	0.58	0.86	0.42	0.43	0.62	0.66	0.70
$^{87}Sr/^{86}Sr$	0.832819	0.753564	0.876049	0.858918	1.005358	0.727531	0.729276
$^{143}Nd/^{144}Nd$	0.511648	0.510579	0.510721	0.510734	0.511226	0.511761	0.511764
ε_{Nd} (0)	-19.3	-40.2	-37.4	-37.1	-27.5	-17.1	-17.0
T_{DM} (Ga)	1.9	3.0	3.0	3.2	2.9	2.1	2.1

	Sukhda Tuff			
Sample ID	CH 15-101C	CH 15-101D	CH 15-101E	CH 15-101F
Sc	1.17	1.6	1.8	1.9
V	3.8	3.8	3.6	3.5
Cr	63	51	54	59
Co	2.4	1.8	1.5	1.24
Ni	1.6	1.17	1.06	0.89
Rb	62	88	80	80
Sr	121	108	111	111
Y	4.1	4.1	3.9	4.0
Zr	86	88	82	87
Nb	16	16	14	15
Cs	4.4	6.1	5.5	5.5
Ba	879	471	378	422
La	39	39	36	35
Ce	81	82	76	73
Pr	8.7	8.9	8.5	8.0
Nd	30.7	31.3	30.8	28.6
Sm	5.5	5.7	5.6	5.3
Eu	1.04	0.95	0.93	0.91
Gd	6.3	6.5	7.2	6.2
Tb	0.53	0.54	0.56	0.52
Dy	1.33	1.36	1.31	1.32
Ho	0.131	0.132	0.126	0.125
Er	0.47	0.49	0.54	0.48
Tm	0.029	0.027	0.029	0.029
Yb	0.272	0.274	0.284	0.274
Lu	0.035	0.032	0.035	0.034
Hf	3.0	3.1	2.9	3.1
Ta	1.40	1.40	1.29	1.38
Pb	13	14	13	13
Th	20	22	19	20
U	1.36	1.37	1.27	1.33
Th/Sc	17	14	10.3	10.3
Zr/Sc	74	56	45	45
La_N/Yb_N	103	103	91	91
Gd_N/Yb_N	19.3	19.5	20.9	18.8
Eu/Eu*	0.54	0.48	0.45	0.48
$^{87}Sr/^{86}Sr$	0.726388	0.732479	0.730437	0.7297 55
$^{143}Nd/^{144}Nd$	0.511723	0.511727	0.511726	0.5117 27
ε_{Nd} (0)	-17.8	-17.8	-17.8	-17.8
T_{DM} (Ga)	2.0	2.0	2.1	2.1

Note: *Silicate fraction in limestone/dolostone. Concentrations are in ppm. External reproducibility of trace element contents is <8% and that of REE's is <3% at 2σ level based on the repeated analysis of BHVO-2. Subscript N indicates concentrations are normalized with Chondritic values. Eu/Eu*= $Eu_N/(Sm_N \times Gd_N)^{0.5}$. ε_{Nd} (0) =

$[(^{143}Nd/^{144}Nd)_{sample}/(^{143}Nd/^{144}Nd)_{CHUR} - 1]x10000$ and was calculated using $(^{143}Nd/^{144}Nd)_{CHUR} = 0.512638$. $f^{Sm/Nd}$ is calculated using present day CHUR value of $^{147}Sm/^{144}Nd = 0.1967$. Depleted Mantle Nd model age (T_{DM}) is calculated using Depleted Mantle reservoir ratios of $^{143}Nd/^{144}Nd = 0.51315$ and $^{147}Sm/^{144}Nd = 0.2137$.